

This Page Is Inserted by IFW Operations
and is not a part of the Official Record

BEST AVAILABLE IMAGES

Defective images within this document are accurate representations of the original documents submitted by the applicant.

Defects in the images may include (but are not limited to):

- BLACK BORDERS
- TEXT CUT OFF AT TOP, BOTTOM OR SIDES
- FADED TEXT
- ILLEGIBLE TEXT
- SKEWED/SLANTED IMAGES
- COLORED PHOTOS
- BLACK OR VERY BLACK AND WHITE DARK PHOTOS
- GRAY SCALE DOCUMENTS

IMAGES ARE BEST AVAILABLE COPY.

As rescanning documents *will not* correct images,
please do not report the images to the
Image Problem Mailbox.

Design of a Potent Combined Pseudopeptide Endothelin-A/Endothelin-B Receptor Antagonist, Ac-DBhg¹⁶-Leu-Asp-Ile-[NMe]Ile-Trp²¹ (PD 156252): Examination of Its Pharmacokinetic and Spectral Properties

Wayne L. Cody,* John X. He, Michael D. Reilly, Stephen J. Haleen, Donneille M. Walker, Eric L. Reyner, Barbra H. Stewart, and Annette M. Doherty

Departments of Chemistry, Vascular and Cardiac Diseases, and Pharmacokinetics & Drug Metabolism, Parke-Davis Pharmaceutical Research, Division of Warner-Lambert Company, Ann Arbor, Michigan 48105

Received March 12, 1997

The endothelins (ETs) are a family of bicyclic 21-amino acid peptides that are potent and prolonged vasoconstrictors. It has been shown that highly potent combined ET_A/ET_B receptor antagonists can be developed from the C-terminal hexapeptide of ET (His¹⁶-Leu¹⁷-Asp¹⁸-Ile¹⁹-Ile²⁰-Trp²¹), such as Ac-ODip¹⁶-Leu-Asp-Ile-Ile-Trp²¹ (PD 142893) and Ac-DBhg¹⁶-Leu-Asp-Ile-Ile-Trp²¹ (PD 145065). However, these compounds are relatively unstable to enzymatic proteolysis as determined in an *in vitro* rat intestinal perfusate assay. This instability is thought to be due to carboxypeptidase activity. In fact, incubation of PD 145065 with carboxypeptidase inhibitors greatly increased its half-life in rat intestinal perfusate. By performing a reduced amide bond and *N*-methyl amino acid scan, it was discovered that *N*-methylation of Ile²⁰ resulted in a compound (Ac-DBhg¹⁶-Leu-Asp-Ile-[NMe]Ile-Trp²¹, PD 156252) that retained full receptor affinity at both endothelin receptor subtypes along with enhanced proteolytic stability and cellular permeability. Interestingly, *N*-methylation of this bond allows the *cis* configuration to be readily accessible which greatly alters the preferred structure of the entire molecule and may be responsible for the observed enhanced metabolic stability.

Introduction

Endothelin-1 (ET-1; Figure 1) is a potent peptidic constrictor of vascular smooth muscle that was first isolated and characterized from the supernatant of porcine endothelial cells.¹⁻³ ET-1 is one member of a family of isopeptides that includes ET-2 and ET-3⁴ along with the structurally and functionally related mouse vasoactive intestinal contractor (VIC),⁵ the cardiotoxic sarafotoxins (SRTXs),^{6,7} and bibrotoxin.⁸ All members of this family possess disulfide bridges between positions 1-15 and 3-11, along with a highly conserved C-terminal hydrophobic hexapeptide, His¹⁶-Xxx-Asp-Yyy-Ile-Trp²¹ (Xxx = Leu or Gln, Yyy = Ile or Val).⁹⁻¹²

Initially, two endothelin receptors were cloned, sequenced, and characterized from the bovine and rat lung, respectively.^{13,14} The ET_A receptor is selective for ET-1 and ET-2 over ET-3, while the ET_B receptor possesses equal affinity for all of the ET isopeptides. Subsequently, the corresponding human receptors have been cloned.^{15,16} The endothelin receptor subtype populations (ET_A/ET_B) are widely distributed in several tissues and possess different functions dependent upon the species and location. For example, a highly selective ET_B receptor ligand, sarafotoxin-6c (SRTX-6c),¹⁷ has linked the ET_B receptor to vasodilation in the rat aortic ring,¹⁸ while it is functionally linked to vasoconstriction in several other tissues.¹⁹ The existence of additional ET_B receptor subtypes and/or species differences has also been reported.²⁰⁻²³

The identification of these receptors has facilitated the development of peptidic and nonpeptidic endothelin

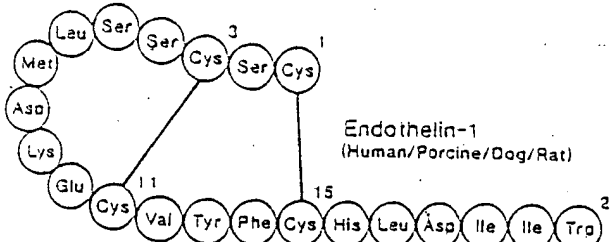


Figure 1. Structure of endothelin-1 (ET-1).

antagonists for the ET_A and ET_B receptors or combined antagonists for both the ET_A and ET_B receptors (for recent reviews, see refs 9-12). This research has focused on a series of combined ET_A/ET_B peptidic antagonists based upon the C-terminal hexapeptide (His¹⁶-Leu-Asp-Ile-Ile-Trp²¹) of the endothelins. In designing these antagonists the importance of the following structural features were considered: (i) the neutralization of the amine terminus by acetylation enhanced activity ~10-fold, (ii) the preference for D-aromatic amino acids in the 16 position, (iii) the requirement for a tryptophan of the L-stereochemistry in the C-terminal 21 position, and (iv) the necessity of a C-terminal carboxylate.²⁴⁻²⁶ These observations resulted in the design and preparation of Ac-ODip¹⁶-Leu-Asp-Ile-Ile-Trp²¹ [compound 2, PD 142893 (Dip = 3,3-diphenylalanine)]^{25,27-29} and Ac-DBhg¹⁶-Leu-Asp-Ile-Ile-Trp²¹ [PD 145065, compound 3 (Bhg = 10,11-dihydro-5H-dibenzo[a,d]cycloheptene-glycine)].³⁰⁻³² Both of these compounds exhibited low-nanomolar affinity for the ET_A (58 and 4.0 nM, respectively) and ET_B (130 and 30 nM, respectively) receptors. Likewise, compounds 2 and 3 were able to antagonize ET-1-stimulated vasoconstriction *in vitro* in the rabbit femoral artery (ET_A, pA₂ = 6.6 and 6.8, respectively) and SRTX-6c-stimulated vaso-

* Author to whom correspondence should be addressed. Phone: (313) 996-7729. Fax: (313) 996-3107. E-mail: codyw@aa.wl.com.

[†] Department of Vascular and Cardiac Diseases.

[‡] Department of Pharmacokinetics & Drug Metabolism.

[§] Abstract published in *Advance ACS Abstracts*, June 15, 1997.

constriction in the rabbit pulmonary artery (ET_B ; $\text{pA}_2 = 6.3$ and 7.0 , respectively).^{25,27-32} Unfortunately, both of these compounds have relatively short half-lives (18.1 ± 3.4 and 10.6 ± 2.2 min, respectively) in rat intestinal perfusate, suggesting limited utility of these compounds for further *in vivo* evaluation.^{33,34}

In an attempt to further stabilize these compounds against proteolytic degradation while maintaining receptor affinity, a reduced amide bond and N-methylated amino acid scan of compound 2 was performed. These modifications, in particular the incorporation of N-methylated amino acids, should have significant effects on the conformational preferences of the peptide backbone. In the case of the N-methylated analogues, the energy barrier between the *cis* and *trans* amide bond conformers is greatly reduced.

In all cases, these modifications, save one, resulted in significant losses of affinity at one or both of the endothelin receptor subtypes. In particular, the incorporation of [NMe]Ile in the 20 position of compound 2 resulted in an analogue, Ac- DDip^{16} -Leu-Asp-Ile-[NMe]-Ile-Trp²¹ (compound 13, PD 149764), that maintained good affinity at both receptor subtypes. This modification was incorporated into the more potent compound 3 template which resulted in an analogue, Ac- DBhg^{16} -Leu-Asp-Ile-[NMe]Ile-Trp²¹ (compound 15, PD 156252), that had high affinity for both receptor subtypes and greatly enhanced pharmacokinetic properties (stability in rat intestinal perfusate and cellular permeability).

In an effort to help understand the reasons for the improved pharmacokinetic properties of compound 15 and, in particular, its conformational preferences with respect to compound 3, an examination of these analogues by $^1\text{H-NMR}$ spectroscopy in solution was performed. One powerful $^1\text{H-NMR}$ technique for the conformational/structural analysis of macromolecules is isotope-edited NMR spectroscopy. This strategy is limited to cases where the soluble macromolecule (in this case, the receptor) is readily available and either it or the ligand can be isotopically enriched with ^{13}C and/or ^{15}N . Unfortunately, in the present scenario this was not the case, since the ET_A and ET_B receptor subtypes were not readily available. A second, more generally applicable, although less powerful, approach is to determine structural parameters of the receptor ligand under a variety of conditions (e.g., solvent, temperature, pH, and the like). If the conformational preferences of the ligand are preserved under several different conditions, there is a reasonable expectation that such conformations are the energetically preferred ones.³⁵ If a compound's three-dimensional structure can survive severe environmental changes, it is even more reasonable to propose that the solution conformation is likely to represent a biologically relevant conformation.

There are several examples of solvent-dependent conformational changes in peptides/pseudopeptides. For example, it is well known from circular dichroism (CD) and NMR studies that fluorinated alcohols, such as trifluoroethanol (TFE) and hexafluoro-2-propanol (HFIP), can induce increased helical structure in linear peptides. There is also abundant literature available describing large conformational changes observed for certain cyclic peptides such as cyclosporin A (CsA) in polar and apolar solvents.³⁶ In fact, it has been shown that the predicted conformation of CsA in lipophilic solvents and the

similar X-ray structure that was suggested to be the bioactive conformation were incorrect using isotope-edited NMR techniques.³⁷ The opposite was shown in the case of rumpamycin, in which the solution structure,³⁷ crystal structure³⁸ and receptor-bound conformations are identical.³⁵ In addition, it has been shown for the cases of the δ receptor selective opioid antagonist [$\text{DPen}^2, \text{DPen}^5$]enkephalin and the cyclic octapeptide known as sandostatin that it is not possible to rely on only the X-ray crystal or solution NMR structure to determine the bioactive structure.^{39,40} In fact, depending upon the particular situation, either method could be argued to be more predictive.

The ability to measure a large number of NMR observables, particularly nuclear Overhauser effects (NOEs), and coupling constants in biomolecules has made possible the determination of several protein structures in solution.⁴¹ It is generally accepted that these data are more abundant and easier to quantitate when internal motion is limited as in the case of medium-sized proteins with extensive secondary and tertiary structure. A much more difficult problem exists, however, when NMR is used to measure the conformational preferences of small peptides in solution. As is often the case in aqueous solution, linear peptides exhibit random coil chemical shifts and yield few structurally relevant NOEs. The lack of NOEs is due to several factors, including multiple conformations and dilution of the intramolecular dipolar interactions by dipolar interactions with solvent. One of the more useful and informative techniques available is analysis of the carbon and proton chemical shifts. Since chemical shifts are sensitive to the peptide backbone angles and the time scale is much faster than for cross-relaxation (10^{-9} versus 10^{-6} s), chemical shifts can yield information on peptides that are undergoing fast exchange between multiple conformations.⁴²

Analysis of the proton NMR characteristics of compound 15 suggested pronounced conformational preferences that were dependent upon the solvent, ionization state, and concentration. For example, in $\text{DMSO}-d_6$, the sodium salt of the peptide adopted a *cis* peptide bond between Ile¹⁹ and [NMe]Ile²⁰, whereas in aqueous solution, this peptide bond was *trans*. In $\text{DMSO}-d_6$ solution the structure was characterized by a wide dispersion in the amide protons with little dispersion in the methyl protons of Ile and Leu. Similar effects were observed by modifying the ionization state or concentration of compound 15 in solution (see below). By comparison, there were not similar spectral changes in compound 3 which lacks the [NMe]Ile²⁰ residue.

Herein, this paper will describe the synthesis of a series of endothelin hexapeptide antagonists based upon compound 3 that contain reduced and N-methylated amide bonds along with structure-activity relationships (SAR) and pharmacokinetic properties. In addition, this manuscript suggests a potential explanation for the increased stability observed in rat intestinal perfusate of compound 15 along with implications to the bioactive conformation of C-terminal endothelin hexapeptide antagonists based upon the measurable NMR parameters.

Chemistry

Peptide Synthesis, Purification, and Characterization. All of the peptide analogues were prepared

Table 1. Binding Affinities (IC_{50} , μM) for Synthetic Analogs of Compounds 2 and 3 at the ET_A and ET_B Receptor Subtypes

Compound No.	Structure	Compound 2 (IC_{50} , μM) ^a	Compound 3 (IC_{50} , μM) ^a	ET_A (\pm SEM) ^b	ET_B (\pm SEM) ^c
2	Ac-Dip ¹⁶ -Leu-Asp-Ile-Ile-Trp ²¹	58	4.0	0.058 \pm 0.01 ^d	0.130 \pm 0.03 ^e
3 ^e	Ac-DBhg ¹⁶ -Leu-Asp-Ile-Ile-Trp ²¹	—	—	0.0040 \pm 0.0004 ^f	0.015 \pm 0.002 ^g
4	Ac-Dip ¹⁶ -(CH ₂ NH)-Leu-Asp-Ile-Ile-Trp ²¹	—	—	2.7 \pm 0.1 ^h	1.3 \pm 0.3 ^h
5	Ac-Dip ¹⁶ -Leu-[CH ₂ NH]-Asp-Ile-Ile-Trp ²¹	—	—	0.26	>0.25
6	Ac-Dip ¹⁶ -Leu-Asp-[CH ₂ NH]-Ile-Ile-Trp ²¹	—	—	0.25	0.020
7	Ac-Dip ¹⁶ -Leu-Asp-[CH ₂ NH]-Ile-Trp ²¹	—	—	0.26	>0.25
8	Ac-Dip ¹⁶ -Leu-Asp-Ile-Ile-[CH ₂ NH]-Trp ²¹	—	—	0.25	>0.25
9	Ac-D(NMe)Dip ¹⁶ -Leu-Asp-Ile-Ile-Trp ²¹	—	—	0.38 \pm 0.01 ^h	>0.25
10	Ac-Dip ¹⁶ -[NMe]Leu-Asp-Ile-Ile-Trp ²¹	—	—	4.5 \pm 0.1 ^h	3.0
11	Ac-Dip ¹⁶ -Leu-[NMe]Asp-Ile-Ile-Trp ²¹	—	—	0.20	0.60
12	Ac-Dip ¹⁶ -Leu-Asp-[NMe]Ile-Ile-Trp ²¹	—	—	3.2	1.5
13 ^h	Ac-Dip ¹⁶ -Leu-Asp-Ile-[NMe]Ile-Trp ²¹	—	—	0.70	>1.0
14	Ac-Dip ¹⁶ -Leu-Asp-Ile-[NMe]Ile-Trp ²¹	—	—	0.030	0.080
15 ⁱ	Ac-DBhg ¹⁶ -Leu-Asp-Ile-[NMe]Ile-Trp ²¹	—	—	3.0	11.0
				0.0010 \pm 0.0003 ^g	0.040

^a Binding data in rabbit renal vascular smooth muscle cells \pm standard error of the mean where more than one IC_{50} was determined.^b Binding data in rat cerebellar membranes \pm standard error of the mean where more than one IC_{50} was determined. ^c PD 142893. ^d PD 145065. ^e n = 15 IC_{50} determinations. ^f n = 19 IC_{50} determinations. ^g n = 4 IC_{50} determinations. All other values represent one IC_{50} determination. IC_{50} values were derived from single competition experiments in which data points were measured in duplicate. Binding data were computer-analyzed by nonlinear least squares analysis giving the best fit for a one-site model. ^h PD 149764. ⁱ PD 156252.

by solid-phase peptide synthetic (SPPS) methodologies.^{43,44} The peptide analogues were prepared utilizing a *tert*-butyloxycarbonyl (*N*^α-*t*-Boc) protecting group strategy on a PAM⁴⁵ (phenylacetamidomethyl) resin. *N*^α-*t*-Boc-protected unusual and *N*-methyl amino acids were purchased from commercial sources or prepared utilizing literature methods.^{46–48} The reduced amide bonds were prepared by reductive amination of the corresponding amino aldehyde.^{49,50} The *N*^α-*t*-Boc-protected amino aldehydes were prepared by reduction of the corresponding *N,O*-dimethylamide ("Weinreb" amides) of the amino acid with lithium aluminum hydride or for aspartic acid by oxidation of the protected amino alcohol.⁵¹ In some cases, *N*-methyl amino acids were prepared on the solid support utilizing a temporary protecting group followed by reductive amination with formaldehyde or for aspartic acid which was prepared in solution by reduction of the corresponding oxazolidinone (see the Experimental Section).^{52,53}

Each *N*^α-*t*-Boc group was removed with 50% trifluoroacetic acid (TFA) in dichloromethane (DCM) and neutralized with 10% diisopropylethylamine (DIEA) in DCM prior to incorporation of the next protected amino acid. All amino acids were single coupled as either their symmetrical anhydrides or *N*-hydroxybenzotriazole (HOBT)-activated esters unless incomplete coupling was indicated, by the Kaiser test.⁵⁴ If incomplete incorporation of the acylating agent was indicated the amino acid was recoupled until a negative Kaiser test was obtained. After coupling of the last amino acid and *N*^α-amine deprotection, the peptide was acetylated with an excess of 1-acetylimidazole in DCM or 10% acetic anhydride in DCM with a catalytic amount of 4-(dimethylamino)-pyridine (DMAP). The peptides were simultaneously deprotected and cleaved from the resin by treatment with anhydrous liquid hydrogen fluoride (HF) and anisole (9:1, v/v) at 0 °C for 1 h. The resin was filtered and washed with diethyl ether, and the crude peptide was extracted into aqueous solution, concentrated under reduced pressure, resuspended in water, and lyophilized.

All crude peptides were purified to homogeneity by preparative reversed-phase high-performance liquid chromatography (HPLC) eluting with a linear gradient of 0.1% aqueous TFA with increasing concentrations of 0.1% TFA in acetonitrile (AcCN). Peptide fractions that

were determined to be homogenous by analytical reversed-phase HPLC were combined and lyophilized. For secondary *in vitro* functional evaluation, the purified peptides were converted to the corresponding disodium salt, by treating the fully protonated analogue with 5% aqueous sodium bicarbonate, followed by solid-phase extraction on a C18 cartridge, elution with methanol, concentration under reduced pressure, resuspension in water, and lyophilization. All final compounds were analyzed for homogeneity by analytical reversed-phase HPLC and/or capillary electrophoresis (CE) and characterized for structural integrity by elemental analysis, electrospray mass spectrometry (FABMS) and proton nuclear magnetic resonance (¹H-NMR) spectroscopy.

Results and Discussion

It has been well documented that potent ET_A and ET_B receptor antagonists can be developed from the C-terminal hexapeptide of endothelin, such as Ac-Dip¹⁶-Leu-Asp-Ile-Ile-Trp²¹ (compound 2, PD 142893)^{25,27–29} and Ac-DBhg¹⁶-Leu-Asp-Ile-Ile-Trp²¹ (compound 3, PD 145065)^{30–32} (Table 1). Both compounds showed similar binding affinities to the ET_A (rabbit renal vascular smooth muscle cells; IC_{50} = 58 and 4.0 nM, respectively) and ET_B (rat cerebellar membranes; IC_{50} = 130 and 15 nM, respectively) receptors. In addition, *in vitro* compound 2 was able to block ET-1-stimulated vasoconstriction in the rabbit femoral artery (ET_A) and sarafotoxin-6c (SRTX-6c)-stimulated vasoconstriction in the rabbit pulmonary artery (ET_B) with pA_2 values of 6.6 and 6.3, respectively.^{25,27–29} Likewise, compound 3 possessed pA_2 values of 6.6 and 6.8 for the ET_A and ET_B receptors, respectively.^{30–32}

Both of these compounds had relatively short half-lives (18.1 ± 3.4 and 10.6 ± 2.2 min, respectively) in rat intestinal perfusate, thus limiting the utility of these compounds for further *in vivo* evaluations.^{33,34} Each compound was degraded to a primary metabolite plus several other fragments under initial rate conditions. Incubation of compound 3 with a carboxypeptidase inhibitor from potato tuber reduced the rate of hydrolysis by 75%. Given that an aromatic amino acid is at the C-terminus of the peptide, this provided evidence of the involvement of carboxypeptidase A which prefers this substrate configuration.⁵⁵ In addition, it was shown by reversed-phase high-performance liquid chromatog-

raphy, as well as mass spectrometry, that Ac-Dip¹⁶-Leu-Asp-Ile-Ile and Ac-DBhg¹⁶-Leu-Asp-Ile-Ile were the primary metabolites of compounds 2 and 3, respectively.^{33,34}

It has been previously shown that N-terminal acetylation of these molecules was required for high receptor affinity; however, modifications of the C-terminus to protect against exopeptidases, such as carboxypeptidases, have not been tolerated.²⁹⁻³¹ In addition, multiple D-amino acid substitutions all led to significant losses of receptor affinity.^{56,57} Thus, we have undertaken a reduced amide and N-methyl amino acid scan of the C-terminal hexapeptide to explore the structural features that will maintain receptor affinity while enhancing stability to enzymatic proteolysis.

Reduced Amide Bond Scan of Compound 2. The reduced amide (aminomethylene) analogues (compounds 4-8) were prepared by reductive amination with the appropriate N^{α} -t-Boc-protected amino aldehyde to the growing peptide on the solid phase or in solution.^{49,50} The protected amino aldehydes were prepared by reduction of the corresponding *N,O*-dimethylamides ("Weinreb" amides) with lithium aluminum hydride or for aspartic acid by oxidation of the protected amino alcohol.⁵¹ Alternatively, the aminomethylene-containing dipeptide was prepared, suitably protected, and coupled directly to the growing peptide (see the Experimental Section). In general, it was observed that the reduced amide analogues (compounds 4-8; Table 1) had 7-70-fold less affinity for the ET_A receptor than the parent peptide (compound 2). Likewise, 4-fold or more loss in binding affinity was observed for the ET_B receptor with respect to compound 2. However, compound 6 with the reduced amide bond between Asp¹³ and Ile¹⁹ actually showed 3-fold enhancement of binding affinity to ET_B with respect to compound 2. In spite of the interesting profile of compound 6, the reduced amide bond series was not pursued further, since the goal of this study was to discover a stabilized ET_A/ET_B receptor antagonist with high affinity for both receptor subtypes, thus a profile similar to that of compounds 2 and 3.

N-Methyl Amino Acid Scan of Compound 2. The mono-*N*-methylated analogues (compounds 9-14) were prepared by incorporation of the N^{α} -t-Boc- or N^{α} -Fmoc-protected *N*-methyl amino acid to the growing peptide on the resin (purchased from commercial sources or prepared by the method of Freidinger et al.⁵³) or by reductive amination on the resin with formaldehyde using a temporary monoprotecting group [4,4'-dimethoxyphenylmethyl (DOD)] on the N^{α} -terminal amine (see the Experimental Section).⁵² Similar to the reduced amide bond analogues, most of the *N*-methylated analogues of compound 2 (compounds 9-12 and 14; Table 1) showed losses in receptor affinity of 7-160-fold. However, Ac-DDip¹⁶-Leu-Asp-Ile-[NMe]Ile-Trp²¹ (compound 13) maintained high affinity for both the ET_A and ET_B receptor subtypes (30 and 80 nM, respectively).³³ [Several conditions were explored [*N,N'*-diisopropylcarbodiimide (DIC), DIC/HOBt, (benzotriazol-1-yl)oxy]tris(dimethylamino)phosphonium hexafluorophosphate (BOP reagent), *O*-(benzotriazol-1-yl)-1,1,3,3-tetramethyluronium hexafluorophosphate (HBTU), and *O*-(7-azabenzotriazol-1-yl)-1,1,3,3-tetramethyluronium hexafluorophosphate (HATU)] for the coupling of Ile¹⁹ to [NMe]Ile²⁰ with little success (<20% incorporation). The use of the

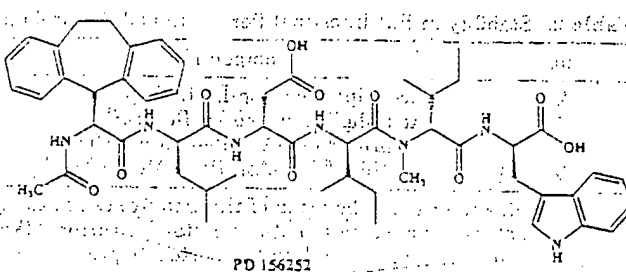


Figure 2. Structure of compound 15 (PD 156252).

acid chloride of N^{α} -Fmoc-Ile proved to be highly effective for this coupling (see the Experimental Section for preparation of compounds 13 and 15).] Also, *in vitro* compound 13 was able to block ET-1-stimulated vasoconstriction in the rabbit femoral artery (ET_A) and SRTX-6c-stimulated vasoconstriction in the rabbit pulmonary artery (ET_B) with pA_2 values of 6.6 and 6.3, respectively.

Due to the profile of compound 13, the $[N^{\alpha}\text{Me}]Ile^{20}$ substitution was incorporated in the more potent Ac-DBhg¹⁶-Leu-Asp-Ile-Trp²¹ (compound 3) template to produce compound 15. Compound 15 showed enhanced binding affinity to both the rabbit ET_A and the rat ET_B receptor subtypes with IC_{50} 's of 1.0 and 40 nM, respectively. Likewise, compound 15 was able to antagonize ET-1-stimulated vasoconstriction *in vitro* in the rabbit femoral artery (ET_A , $pA_2 = 7.3$) and SRTX-6c-stimulated vasoconstriction in the rabbit pulmonary artery (ET_B , $pA_2 = 6.6$). Thus, compound 15 represents a highly potent combined ET_A and ET_B receptor antagonist (Figure 2).³³

It has been previously reported that a significant species difference between the binding affinity of ligands for endothelin receptors can exist, especially in the case of the ET_B receptor. In general, compounds have been shown to possess significantly lower affinity (150-fold and greater) for the human cloned ET_B receptor than for the corresponding rat receptor.^{22,23,29} Compound 15 maintained good binding affinity for both the human cloned ET_A and ET_B receptor subtypes (3.0 and 25 nM, respectively).

As shown previously, the parent compounds 2 and 3 were unstable in rat intestinal perfusate with half-lives of 18.1 ± 3.4 and 10.6 ± 2.2 min, respectively.^{33,34} Large increases in the half-lives of the $[N^{\alpha}\text{Me}]Ile^{20}$ analogues (PD 149764 and PD 156252) were observed. In fact, compounds 13 and 15 were approximately 50-fold more stable than their parent analogues with half-lives in rat intestinal perfusate of 875 ± 145 and 538 ± 52 min, respectively (Table 2).

Caco-2 cells are a continuously cultured cell line derived from human colon adenocarcinoma that spontaneously differentiate to resemble the epithelial cells that line the small intestine and have been widely used as an *in vitro* model of intestinal absorption.⁵⁶⁻⁵⁸ Several of the hexapeptide antagonists were examined in this model: compounds 2, 3, 13, and 15. All of these compounds are of similar molecular weight and charge (-2 at physiological pH). The Caco-2 permeabilities of the hexapeptide ET antagonists ranged from approximately 2.0×10^{-4} to 6.3×10^{-4} cm/min which, when compared to standard compounds, suggests a potential for moderate, but measurable, intestinal absorption *in vivo* in the range of 5-10% (Table 2). Compound 2 was the least permeable, and compound 15 was clearly the

Table 2. Stability in Rat Intestinal Perfusion and Permeability in Caco-2 Cell Monolayers for Compounds 2, 3, 13, and 15

no.	compound	permeability ^a (10 ⁴ , cm/min)	stability ^b (h)
2 ^c	Ac-Dip ¹⁶ -Leu-Asp-Ile-Ile-Trp ²¹	2.0 ± 0.5	18.1 ± 3.4
3 ^d	Ac-DBhg ¹⁶ -Leu-Asp-Ile-Ile-Trp ²¹	4.7 ± 0.9	10.6 ± 2.2
13 ^e	Ac-Dip ¹⁶ -Leu-Asp-Ile-[NMe]Ile-Trp ²¹	2.0 ± 0.8	875 ± 145
15 ^f	Ac-DBhg ¹⁶ -Leu-Asp-Ile-[NMe]Ile-Trp ²¹	6.3 ± 2.5	538 ± 52

^a Each value represents the mean of three to five cell monolayers. Standard errors are tabulated with the mean values. ^b Values are the mean of at least three determinations ± standard error of the mean from two perfusate preparations. Leucine aminopeptidase activity ranged from 0.05 to 0.32 nkat/mL in the perfusate preparations. ^c PD 142893. ^d PD 145065. ^e PD 149764. ^f PD 156252.

most permeable. This increase in permeability is likely due to the enhanced lipophilicity of compound 3. However, the differences between analogues were small and the permeabilities were low, as could be anticipated from the physicochemical properties described above.

In addition, compound 15 was shown to possess *in vivo* activity by inhibition of the pressor response to an ET-1 challenge in a conscious rat model. In particular, a dose of 10 mg/kg of compound 15 was administered iv bolus to conscious rats 5 and 30 min prior to an ET-1 challenge (0.30 nM/kg, iv bolus). Compound 15 was shown to reduce the pressor response to ET-1 by 81% and 58%, respectively. Thus, compound 15 was effective as an antagonist in an *in vivo* model in a time dependent manner.

NMR Studies of Compounds 3 and 15. The following discussion involves a description of (1) the ¹H-NMR spectral properties of compounds 3 and 15 under various conditions including solvent content and ionization state and (2) the structural properties of two different conformations of the sodium salt of compound 15. Under each different set of conditions employed, rigorous proton NMR assignments were made using well-established 2D procedures.⁴¹ The ¹H-NMR spectral parameters of compound 3 have been previously reported in dodecylphosphocholine micelles.⁶¹ In micelles, compound 3 was shown to adopt a standard turn topology in three closely related families which were significantly different than the structures observed in aqueous or DMSO-*d*₆ solution. In addition, it was shown that compound 3 was in fast chemical exchange between several closely related conformational states.⁶¹ The proton NMR data for the disodium salt and fully protonated forms of compounds 3 and 15 in aqueous and DMSO-*d*₆ solution are provided in the Supporting Information.

Effect of Solvent on Spectral Characteristics. The 1D ¹H-NMR spectra of the disodium salt forms of compounds 3 (3-Na) and 15 (15-Na) in DMSO-*d*₆ (top trace) and aqueous (bottom trace) solution are shown in Figure 3A,B, respectively. In the case of compound 3-Na, the ¹H-NMR spectrum is slightly different in the two solvents, with small changes in chemical shift dispersion in most regions of the spectrum (Figure 3A).

However, the ¹H-NMR spectra of compound 15-Na in DMSO-*d*₆ and aqueous solution are significantly different from each other (Figure 3B). The DMSO-*d*₆ spectrum (top trace) is characterized by significant spectral dispersion of the amide protons, aspartic acid β protons, and a clustering of the methyl protons of the leucine and isoleucine residues. However, the aqueous spectrum (bottom trace) is characterized by a large degree of dispersion in the methyl region, with the γ methyl protons of Ile¹⁹ at exceptionally high field (0.18 ppm). Other regions of the spectrum are more similar to each other. Interestingly, addition of 10% (v/v) water to a

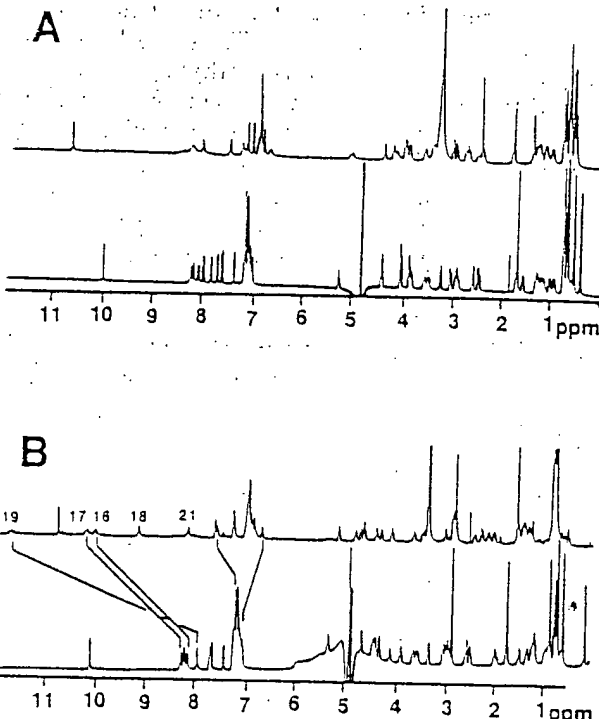


Figure 3. 500 MHz ¹H-NMR spectra of compound 3-Na (A) and compound 15-Na (B). In both cases, the bottom trace is the peptide dissolved in 90% H₂O/10% D₂O with the pH adjusted to 6.7 and the top trace is the peptide dissolved in DMSO-*d*₆.

solution of compound 15-Na in DMSO-*d*₆ caused a collapse of the dispersion in the amide region and an increase in dispersion in the methyl region of the spectrum such that the spectrum becomes similar to the aqueous spectrum (data not shown). In the converse experiment, addition of up to 50% (v/v) DMSO-*d*₆ to an aqueous solution of compound 15-Na resulted in a slight increase in the dispersion in the amide protons and a decrease in the spread of the methyl proton chemical shifts of leucine and isoleucine. These dramatic differences in the ¹H-NMR spectral properties of compound 15-Na that are solvent dependent are most likely due to *cis* = *trans* isomerization around the Ile¹⁹-[NMe]Ile²⁰ amide bond.

To further investigate this phenomenon, the ¹H-NMR spectrum was qualitatively analyzed for compound 15-Na in a number of other organic solvents (data not shown). The spectrum of compound 15-Na in methanol-*d*₃ solution was similar to the peptide dissolved in aqueous solution, whereas the spectrum in DMF-*d*₇ was very nearly identical to that observed in DMSO-*d*₆. The peptide dissolved readily in acetone-*d*₆ and sparingly in AcCN-*d*₃. The resonances were extremely broad in both solvents, suggesting extensive aggregation.

Secondary Chemical Shifts. It has been well established that proton and carbon chemical shifts in

peptides and proteins are sensitive to Φ and Ψ angles.⁵² Thus, the secondary Ca and Ha chemical shifts for both forms of compounds 3 and 15 were analyzed. The fully protonated peptides dissolved in $\text{DMSO}-d_6$ show only small secondary shifts, indicative of highly flexible conformation properties. For the two analogues in D_2O , a similar secondary shift pattern is observed for compounds 3-Na and 15-Na, with the main difference being a larger negative secondary shift at position 19 in the N-methylated peptide (compound 15-Na). In $\text{DMSO}-d_6$, both peptides clearly become more ordered, but their secondary shifts now differ significantly in both magnitude and sign. Interestingly, the major difference between the disodium peptides in $\text{DMSO}-d_6$ is again at Ile^{19} , with a ~5 ppm difference in secondary shift and a change in sign. Also, the magnitudes of the secondary shifts for compound 15-Na are universally higher than for compound 3-Na, suggesting a more stable secondary structure for the methylated peptide.

Quantitative analysis of these secondary shifts is complicated by several factors. First, in our analysis of Gly-Gly-[NMe]Ile-Gly-Gly, only the *trans* conformer was observed in aqueous and $\text{DMSO}-d_6$ solutions. Therefore, the appropriate random coil chemical shift is not available for the *cis* conformation of [NMe]Ile. Hence, the random coil chemical shift for the *trans* conformation was used for all peptides. This may be a reasonable value, since it is known that Pro Ca shifts are not very sensitive to the geometric configuration about the imide bond. Second, the nearest-neighbor corrections for the random coil chemical shift of Ile^{19} (when preceding [NMe]Ile) were taken from work with proline-containing peptides.⁶³ Here again, the assumption that [NMe]Ile is similar to proline with respect to secondary shifts may not be valid.

Effect of Ionization State. The $^1\text{H-NMR}$ spectrum of the fully protonated form of compound 15 in $\text{DMSO}-d_6$ is characterized by poor dispersion with very little indication of secondary structure. The temperature coefficients and amide to α proton coupling constants ($^3J_{\text{NHHA}}$, Table 2) that can be measured are consistent with a conformationally flexible structure. Addition of 20% aqueous sodium hydroxide in approximately equimolar proportional steps initially results in a broadening of the signals in the amide region, and two sets of signals could be seen for some of the aliphatic protons. This is most likely due to *cis* = *trans* isomerization around the Ile^{19} -[NMe]Ile²⁰ amide bond induced by deprotonation of the peptide, *vide infra*. Addition of a third equivalent of base resulted in a spectrum essentially identical with that of compound 15-Na. When a similar titration was performed with aqueous potassium hydroxide or cesium hydroxide, the results were indistinguishable from those using NaOH.

The above results are consistent with the following hypotheses/observations: Firstly, a distinct conformation is observed for compound 15-Na in aprotic anhydrous solvents ($\text{DMSO}-d_6$, etc.) that is "more ordered" than the conformation observed in protic solvents or that of the protonated peptide species in aprotic solvents. Thus, the "ordered" structure is not favored when the C-terminal and aspartic acid side chain carboxyl anions are fully or partially neutralized by protons or efficient solvation. Secondly, this "ordered" structure is not readily accessible to an analogue of

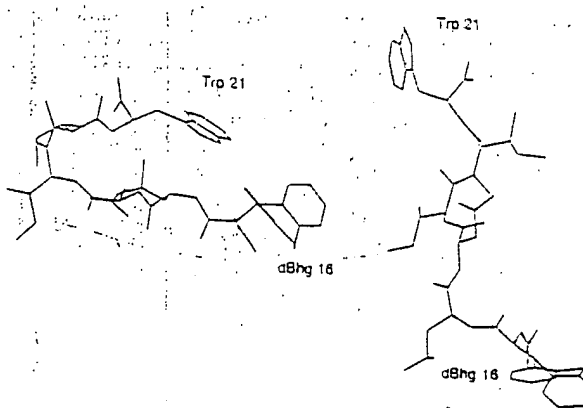


Figure 4. Structures of *cis* (left) and *trans* (right) conformers of compound 15.

compound 15-Na that does not contain an [NMe]Ile²⁰, (i.e., compound 3-Na).

Conformational Preferences for Compound 15-Na. Because of the unique spectral features observed for compound 15 (but not compound 3), the hypothesis that the structure characterized by the unusually large dispersion of amide proton chemical shifts was due to the formation of a *cis* peptide bond between Ile¹⁹ and [NMe]Ile²⁰ was investigated. Methylation of the amide of Ile²⁰ decreases the energy difference between the *trans* and *cis* configurations, making both energetically accessible. NOEs between the α protons of Ile¹⁹ and Ile²⁰ or [NMe]Ile²⁰ established that, indeed, the sodium form of the peptide was 100% *cis* (about the Ile¹⁹-[NMe]Ile²⁰ peptide bond) in $\text{DMSO}-d_6$, while the lack of NOEs in aqueous solution established that the peptide bond was 100% *trans*.

In one 15 mM sample of compound 15-Na in $\text{DMSO}-d_6$, numerous medium and long range NOEs in a NOESY spectrum recorded with a mixing time of 400 ms were observed. The sign of the NOEs was consistent with a correlation time of greater than 1 ns, which was somewhat surprising for a linear hexapeptide. To investigate this further, NOESY spectra were obtained at 80, 120, and 200 ms, respectively. Analysis of the NOE buildup curves provided clear evidence that many of the cross-peaks observed in the 400 ms NOESY were due to spin diffusion. Analysis of the shapes of the buildup curves suggested that all of the NOE information in the 80 ms NOESY was due to direct cross-relaxation. Sixty-five cross-peak volumes were converted to upper bound distance constraints and used to generate structures for compound 15-Na. In addition to distance constraints, the Φ angles of residues 16, 17, and 19 were constrained to the range of -75° to -175° , based on $^3J_{\text{NHHA}}$.

Using these constraints, 20 structures were generated by distance geometry/simulated annealing. Nineteen of these had final DGII optimization errors of <0.1 , and none of these had experimental distance violations of more than 0.3 Å. Representative structures from these calculations are shown in Figure 4.

Several structural features that were consistent with the observed spectral properties were apparent. First, the close proximity of Leu¹⁷ and Ile¹⁹ side chains to the dBhg¹⁶ and Trp²¹ side chains, respectively, could explain the high-field-shifted methyl protons observed in the *trans* conformer. These were also consistent with the aromatic methyl NOEs observed for compounds 3-Na

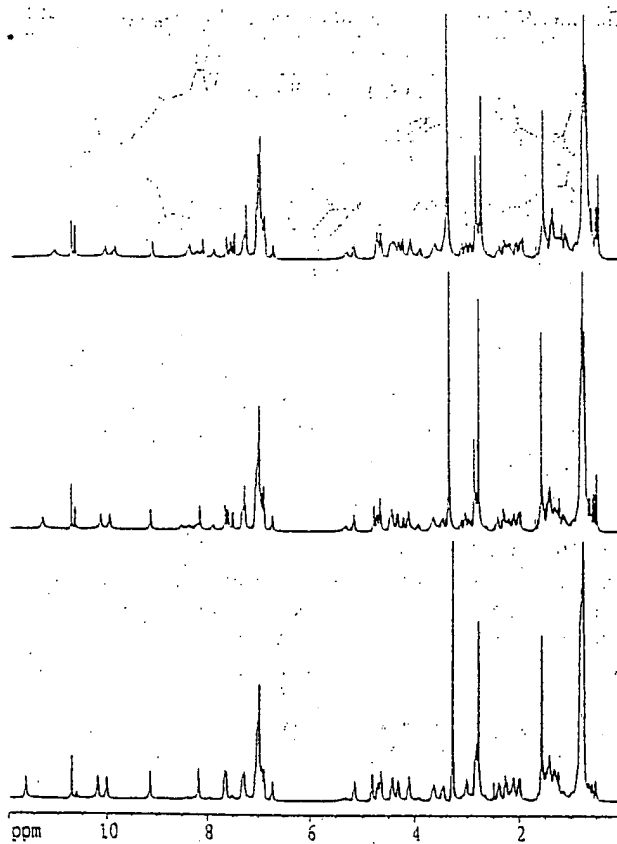


Figure 5. Concentration dependence of the ^1H -NMR spectrum of compound 15·Na in $\text{DMSO}-d_6$ at 35°C . The three concentrations shown are 145 mM (top trace), 72 mM (middle trace), and 36 mM (bottom trace).

and 15·Na in aqueous solution and for the fully protonated forms of compounds 3 and 15 in $\text{DMSO}-d_6$. In the structures calculated for compound 15·Na in $\text{DMSO}-d_6$, the three aliphatic side chains were exposed to solvent and further removed from the aromatic side chains, consistent with the lack of chemical shift dispersion for these species. Second, although the side chain of Trp for compound 15·Na was not well defined in the ensemble of structures, on average it was closer to the DBhg¹⁶ side chain than in the extended structure. Mutual ring current effects could be invoked to explain the additional dispersion in the aromatic resonances of the DBhg¹⁶ residue and the unusual chemical shifts of the Trp²¹ side chains (compared to Trp in a random coil peptide) for the sodium salt in $\text{DMSO}-d_6$. Third, the amide protons were internalized in the calculated structures, consistent with their highly disperse chemical shifts and relatively small temperature coefficients. Finally, the C-terminal carboxylate was poised for hydrogen-bonding interactions with the NH of Ile¹⁹ and/or Asp¹⁸ in many of the final structures. The potential for electrostatic interaction between the C-terminal carboxylate and amide protons could be a driving force for *cis*-peptide bond formation in this peptide dissolved in an aprotic solvent. Possible structures for the *cis* and *trans* conformers of compound 15·Na are shown in Figure 4.

Concentration Dependence of Compound 15·Na in $\text{DMSO}-d_6$ Solution. In an attempt to measure the three bond $^{13}\text{C}_\beta\text{-NH}$ coupling constants, a sample was prepared by dissolving 72 mg of compound 15·Na in 0.5 mL of $\text{DMSO}-d_6$ (~ 150 mM). The resulting spectrum was more complex than expected based upon spectra

recorded at lower concentrations. Diluting this sample 4-fold resulted in a return to a more normal spectrum (Figure 5). Some resonances (cf. the Trp indole resonances at 10.6 ppm) suggest a slow exchange between different species, whereas the amide protons simply broaden and/or move to higher field at the higher concentration. A possible explanation for the concentration-dependent behavior of the spectrum is a monomer = multimer equilibrium or an ionic strength/pH effect. The peak positions of the species that forms at higher concentrations are similar to those observed for the fully protonated form of compound 15, suggesting that this species contains compound 15 in the *trans* configuration.

Addition of substoichiometric amounts of sodium hydroxide to a 60 mM solution of the fully protonated form of compound 15 resulted in a decrease in the amount of this species with a concomitant increase in the species identified as the *cis* configuration of compound 15·Na. Thus it appears that the second species observed at higher concentrations may be the *trans* configuration of compound 15 and that its relative abundance may be a function of the effective pH and/or ionic strength in the $\text{DMSO}-d_6$ solution. This is affected by such difficult to control variables as the extent of hydration and the exact protonation state of the peptide, as well as the amount of water present in the solvent.

Conclusions

Compound 15 represents a constrained analogue of compound 3 that is a highly potent combined ET_A and ET_B receptor antagonist. Compound 15 showed enhanced binding affinity to both the rabbit ET_A and rat ET_B receptor subtypes with IC_{50} 's of 1.0 and 40 nM, respectively). Likewise, compound 15 was able to antagonize ET-1-stimulated vasoconstriction *in vitro* in the rabbit femoral artery (ET_A , $\text{pA}_2 = 7.3$) and SRTX-6c-stimulated vasoconstriction in the rabbit pulmonary artery (ET_B , $\text{pA}_2 = 6.6$). In addition, compound 15 was approximately 50-fold more stable than compound 3 in rat intestinal perfusate with a half-life greater than 500 min. Since the only difference between compounds 3 and 15 lies in the N-methylation of the amide bond between Ile¹⁹ and Ile²⁰, the enhanced proteolytic stability and cellular permeability must be related physically or conformationally to this modification. In addition, since N-methylation of an amide bond is known to have significant effects on the conformational preferences of the peptide backbone and compound 15 is a highly potent analogue, it must be assumed that this modification has constrained the molecule in a conformation that is favored for interaction with the ET receptor subtypes.

It is intriguing to speculate that the enhanced stability of compound 15 may be a result of the energetically favored accessibility of the *cis* amide bond conformer. From the above ^1H -NMR studies it had been shown that in aqueous solution compound 15·Na exists exclusively in the *trans* amide bond form; however, upon the addition of $\text{DMSO}-d_6$ the *cis* form became accessible. The *cis* form was also shown to depend upon the ionization state of compound 15. Based upon these results it was obvious that the energy barrier between the *trans* and *cis* conformers is low and readily obtainable; thus it was not possible to predict the preferred structure of compound 15 under physiological conditions. If the *cis* conformer was predominant, it can be

seen from Figure 4 that C-terminal carboxylate would be buried and less accessible to carboxypeptidase activity, accounting for the increased stability of compound 15 in rat intestinal perfusate. In the same regard, it is possible that methylation of the p-1 amino acid of a carboxypeptidase substrate may lead to an analogue that does not fit properly into the enzyme, either sterically or simply by disruption of a critical hydrogen-bonding interaction. Resolution of the exact reasons for the increased stability will require additional studies, which are not the focus of this manuscript. Such studies could include replacement of the $\text{Ile}^{19}-[\text{NMe}]\text{Ile}^{20}$ amide bond with peptidomimetic isosteres (*cis* alkenes and the like) that would lock the molecule into the *cis* configuration.

It is also quite intriguing that the simple modification of N-methylating a single amide bond of a hexapeptide can have such profound effects on the intrinsic stability of the molecule in rat intestinal perfusate without concomitant effects on cellular permeability. In this regard, it should become common practice in the development of second-generation peptidomimetic compounds designed from a peptide lead for extended *in vitro* and *in vivo* evaluations to perform a reduced amide bond and N-methylated amino acid scan. As can be seen from above, this can impart desirable physicochemical properties into the molecule as well as provide insights into the understanding of the bioactive conformation.

Experimental Section

Materials and Methods. Orthogonally protected $\text{N}^{\alpha}\text{-t-Boc}$ amino acids, $\text{N}^{\alpha}\text{-Fmoc}$ amino acids, and $\text{N}^{\alpha}\text{-t-Boc-Trp-PAM}$ resins were purchased from either Advanced Chemtech, Applied Biosystems Inc., Bachem California, Bachem Bioscience, Novabiochem, Peninsula Laboratories, Inc., or Synthetech Inc. All amino acids were of the *L*-configuration unless otherwise noted.

TFA was purchased from Halocarbon. *N,N*'-Dicyclohexylcarbodiimide (DCC), DIEA, and HOBT were purchased from Applied Biosystems Inc. (ABI). *N,N*-Dimethylformamide (DMF), DCM, and NMP were purchased from Burdick & Jackson and were of reagent grade or better. HPLC grade solvents (AcCN and water) were obtained from Burdick and Jackson, EM Science, or Mallinckrodt. HF was purchased from Matheson Gas Products. All of the other reagents for chemical synthesis were purchased from Aldrich Chemical Co., Inc. or similar suppliers. Tris(hydroxymethyl)aminomethane (Trizma), ethylenediaminetetraacetate (EDTA), and *N*-(2-hydroxyethyl)piperazine-*N'*-(2-ethanesulfonic acid) (HEPES) were purchased from Sigma Chemical Co. Phenylmethanesulfonyl fluoride (PMSF) and bacitracin were purchased from Boehringer Mannheim Biochemicals. Bovine serum albumin (BSA) was purchased from Miles Inc., Diagnostics Division. [^{125}I]ET-1 (2000 Ci/mmol) was purchased from New England Nuclear, DuPont and [^3H]arachidonic acid (218 Ci/mmol) was purchased from Amersham.

The peptides were prepared on an ABI Model 430A or 431A peptide synthesizer using software version 1.40. For $\text{N}^{\alpha}\text{-t-Boc}$ syntheses, the HF cleavages were performed on an Immuno-Dynamics Inc. Model 2A/2B HF Apparatus. High-pressure liquid chromatographs were obtained on a Waters HPLC system from Millipore Corp. equipped with a Model 600E system controller, a Model 600-solvent delivery system, a Model 490 variable wavelength detector operating at 214 and 280 nm, and a Bio-Rad Laboratories Model AS-100 autosampler. Vydac analytical and preparative C18 HPLC columns were purchased from The Nest Group. Preparative reversed-phase HPLC was performed using a C18 preparative scale Vydac column (218TP1022) (2.2 \times 25.0 cm, 10–20 mM particle size) eluting with a linear gradient of 0.1% aqueous TFA with increasing concentrations of AcCN at 15 mL/min. Analytical

reversed-phase HPLC analysis was carried out on a Vydac column (218TP54) (0.46 \times 25.0 cm, 5 μm particle size). The analytical HPLC system used was the same as that described in detail above for peptide purification. The mobile phase utilized for the analytical HPLC analysis was 80% A:20% B to 14% A:86% B [0.1% aqueous TFA (A):0.1% TFA in AcCN (B)]; linear gradient was over 22 min at 1.5 mL/min (λ = 214 and 280 nm) on a Vydac 218TP54 column.

Chemical ionization mass spectra (CIMS) were acquired with a Fisons VG Trio-2A quadrupole mass spectrometer using 1% ammonia in methane as the reagent gas. Fast atom bombardment mass spectra (FABMS) were measured with a VG analytical 7070E/HF mass spectrometer in either a thioglycerol or 3-nitrobenzyl alcohol matrix using xenon as the target gas. Electrospray mass spectra (ESMS) were obtained on either a Finnigan TSQ70 or Fisons VG Trio 2000 quadrupole mass spectrometer using 50:50 water:methanol made 1% in acetic acid as the solvent. Routine $^1\text{H-NMR}$ spectra were measured with a Varian Gemini 2300 or Varian Unity 400 instrument using tetramethylsilane as an external standard in chloroform or dimethyl sulfoxide (CDCl_3 or $\text{DMSO-}d_6$; Cambridge Isotope Laboratories).

[^{14}C]PEG-4000 was purchased from New England Nuclear, DuPont (NEN). Reference compounds that were used to establish the correlation between fractions absorbed in humans and transport across CACO-2 cell monolayers were either obtained from Sigma Chemical Co., with the radiolabeled form of the compounds purchased from NEN (*D*-mannitol, hydrocortisone, phenytoin, and *L*-phenylalanine), or synthesized at Parke-Davis (gabapentin and cefdinir). Modified MES buffer was prepared from MES [2-(*N*-morpholino)ethanesulfonic acid], NaCl, and KCl (Sigma Chemical Co.). *D*-Glucose and human serum albumin were also purchased from Sigma. Anesthetics used included Ketaset (ketamine HCl injection, USP, 100 mg/mL; Aveco Co., Inc.), Rompun (xylazine, 20 mg/mL; Miles Inc.), and sodium pentobarbital (64.8 mg/mL; Anthony Products) for all animal surgery.

General Strategy: 1. **Peptide Synthesis.** All of the peptides were synthesized by solid-phase peptide synthetic techniques on an ABI Model 430A or 431A peptide synthesizer. The peptide analogues were prepared using an $\text{N}^{\alpha}\text{-t-Boc}$ protection scheme with $\text{N}^{\alpha}\text{-t-Boc-Trp-PAM}$ resin and the aspartic acid side chain carboxylate protected as the benzyl ester. Individual $\text{N}^{\alpha}\text{-t-Boc}$ amino acids were coupled via DCC in DMF. Deprotection of the $\text{N}^{\alpha}\text{-t-Boc}$ group was achieved with 50% TFA in DCM, and removal of the $\text{N}^{\alpha}\text{-Fmoc}$ group was accomplished with 20% piperidine in DCM. N-Terminal acetylation was carried out on the resin in DCM with an excess of 1-acetylimidazole (20-fold) or 10% acetic anhydride in DCM with a catalytic amount of DMAP. The resin was then washed in turn with DMF, MeOH, and DCM (2 \times each) and dried under reduced pressure. The peptides were then deprotected and cleaved from the resin using anhydrous liquid HF:anisole (9:1). The resin was washed with anhydrous ethyl ether, and the crude peptide was extracted from the resin with AcCN:water (1:1) with 0.1% TFA, concentrated under reduced pressure, and lyophilized. (See ref 27 for the detailed solid-phase synthesis of compound 2, which is representative of all solid-phase syntheses in this report.)

2. **Peptide Purification.** Crude peptides were dissolved in a mixture of aqueous 0.1% TFA and AcCN (exact ratio depending on the solubility of the peptide) and then purified by preparative reversed-phase HPLC (see above). Peptide fractions determined to be pure by analytical HPLC were combined, concentrated under reduced pressure, and lyophilized.

3. **Peptide Homogeneity and Characterization.** Peptides were assessed for homogeneity by analytical reversed-phase analytical HPLC. The peptides were characterized by ESMS or FABMS and $^1\text{H-NMR}$ spectroscopy. All final peptidomimetic compounds (4–15) provided an $^1\text{H-NMR}$ spectrum that was consistent with the desired structure; however, due to the complexity of the resulting spectrum individual assignments are not provided.

Preparation of $\text{Ac-D}\text{Dip-}\Psi[\text{CH}_2\text{NH}]\text{-Leu-Asp-Ile-Ile-Trp}$ (4). Preparation of $\text{N}^{\alpha}\text{-t-Boc-D}\text{Dip-N}(\text{CH}_3)\text{OCH}_3$. To

a solution of N^{α} -*t*-Boc- α Dip (3.0 g, 3.0 mmol) in DMF (20 mL) were added HCl- $\text{HN}(\text{CH}_2\text{OCH}_3)_2$ (0.5 g, 8.3 mmol), and DIEA (3.0 mL, 17.2 mmol) followed by BOP reagent (3.9 g, 8.8 mmol). The reaction was allowed to continue for 2 h. The reaction mixture was then concentrated to dryness. The residue was taken up with ethyl acetate (EtOAc; 50 mL), washed with saturated aqueous Na_2CO_3 (2 \times 50 mL), water, and 1 M aqueous KHSO_4 (2 \times 50 mL), dried over MgSO_4 , and concentrated under reduced pressure to yield a white foam (3.3 g, 88%): $^1\text{H-NMR}$ (CDCl_3) δ 1.31 (s, 9H), 2.94 (s, 3H), 3.61 (s, 3H), 4.32 (d, 1H), 4.99 (d, 1H), 5.68 (t, 1H), 7.27 (m, 10H); CIMS (m/z)⁺ calcd 384.2, found 385 (M + H).

Preparation of N^{α} -*t*-Boc- α Dip-CHO. To a solution of N^{α} -*t*-Boc- α Dip- $\text{N}(\text{CH}_3\text{OCH}_3)_2$ (3.3 g, 8.5 mmol) in dry THF (50 mL) at 0 °C, was added, in portions, lithium aluminum hydride (0.43 g, 11.1 mmol). The reaction was allowed to continue for 30 min at 0 °C and was quenched by adding 1 M aqueous KHSO_4 (20 mL). The organic phase was separated and the aqueous phase extracted with EtOAc (50 mL). The combined organic layer was washed with brine, dried with MgSO_4 , and concentrated under reduced pressure to give a colorless oil which crystallized on standing at room temperature (2.75 g, 99%): $^1\text{H-NMR}$ (CDCl_3) δ 1.39 (s, 9H), 4.50 (d, 1H), 4.88 (d, 1H), 5.07 (t, 1H), 7.28 (m, 10H), 9.61 (s, 1H); CIMS (m/z)⁺ calcd 325.4, found 326 (M + H).

Preparation of Ac- α Dip- $\Psi[\text{CH}_2\text{NH}]\text{-Leu-Asp-Ile-Ile-Trp}$ (4). The synthesis of N^{α} -*t*-Boc-Leu-Asp-Ile-Ile-Trp-PAM resin was performed as described in the general procedure on a 1.0 mmol scale. N^{α} -*t*-Boc-Leu-Asp-Ile-Ile-Trp-PAM resin was treated with 50% TFA in DCM (20 mL) for 30 min at room temperature and washed successively with DCM (3 \times 20 mL), 10% DIEA in DCM (20 mL), DMF (3 \times 20 mL), and 5% acetic acid in DMF (2 \times 20 mL). N^{α} -*t*-Boc- α Dip-CHO (1.2 g, 3.0 mmol) was added followed by 1% acetic acid in DMF (20 mL) and 1 M NaBH_3CN -THF (3.3 mL, 3.3 mmol). The mixture was shaken at room temperature for 3 h. The resin was then washed in turn with DMF, MeOH, and DCM (2 \times 20 mL, each) and dried under reduced pressure. The peptide was deprotected and cleaved from the resin using anhydrous HF as described in the general procedure. The crude peptide was purified by reversed-phase HPLC to afford 230 mg of the title compound: HPLC t_R = 12.5 min (>99%); ESMS (m/z)⁺ calcd 910.1, found 910.6 (M).

Preparation of Ac- α Dip-Leu- $\Psi[\text{CH}_2\text{NH}]\text{-Asp-Ile-Ile-Trp}$ (5). Preparation of N^{α} -Benzylloxycarbonyl(Cbz)-Leu- $\Psi[\text{CH}_2\text{NH}]\text{-Asp(OBu')-OBzI}$. N^{α} -Cbz-Leu-CHO was prepared in two steps from N^{α} -Cbz-Leu as described for N^{α} -*t*-Boc- α Dip-CHO (30.8 g, 99%): $^1\text{H-NMR}$ (CDCl_3) δ 0.95 (m, 6H), 1.74 (m, 3H), 4.38 (m, 1H), 5.12 (s, 2H), 5.38 (m, 1H), 7.34 (s, 5H), 9.60 (s, 1H); CIMS (m/z)⁺ calcd 249.3, found 250 (M + H).

N^{α} -Cbz-Leu-CHO (14.5 g, 58 mmol) was dissolved in dry MeOH (500 mL) and treated with H-Asp(OBu')-OBzI-HCl (16.2 g, 58.0 mmol) followed by NaBH_3CN (3.77 g, 60.1 mmol) and acetic acid (HOAc; 4.0 mL, 66.5 mmol). The reaction was allowed to continue overnight and concentrated under reduced pressure to dryness. The residue was taken up with EtOAc (200 mL); the organic layer was washed with saturated NaHCO_3 and brine, dried with MgSO_4 , and concentrated under reduced pressure to an oil (15.1 g, 52%): $^1\text{H-NMR}$ (CDCl_3) δ 0.89 (m, 6H), 1.28 (m, 1H), 1.40 (s, 9H), 1.52-2.51 (m, 4H), 2.75 (m, 4H), 3.75 (m, 2H), 5.08 (s, 2H), 5.17 (s, 2H), 7.32 (m, 10H); CIMS (m/z)⁺ calcd 512.3, found 513 (M + H).

Preparation of N^{α} -Fmoc-Leu- $\Psi[\text{CH}_2\text{NH}]\text{-Asp(OBu')}$. N^{α} -Cbz-Leu- $\Psi[\text{CH}_2\text{NH}]\text{-Asp(OBu')-OBzI}$ was dissolved in MeOH (200 mL), treated with 20% Pd/C (2.0 g), and placed under a hydrogen atmosphere at 50 psi (2 h, room temperature). The reaction mixture was filtered through a Celite pad, and solvent was evaporated under reduced pressure to provide a white solid (6.0 g, 71%) which was suspended in a mixture of *p*-dioxane:water (1:1, 200 mL). The solution was treated with triethylamine (7.35 mL, 52.8 mmol) followed by 9-fluorenylmethyloxycarbonyl-N-hydroxysuccinimide (Fmoc-OSu, 7.0 g, 20 mmol). The solution was stirred at room temperature overnight and treated with 1 M aqueous KHSO_4 (52.0 mL), and the precipitate was collected by filtration (6.4 g, 55% yield): $^1\text{H-NMR}$ ($\text{DMSO}-d_6$) δ 0.82 (m, 6H), 1.18 (m, 1H), 1.40

(s, 9H), 1.48 (m, 4H), 2.95 (m, 5H), 3.88 (m, 1H), 4.22 (m, 3H), 4.54 (m, 1H), 7.32 (m, 2H), 7.63 (m, 2H), 7.88 (m, 2H); FABMS (m/z)⁺ calcd 510.2, found 511 (M + H).

Preparation of Ac- α Dip-Leu- $\Psi[\text{CH}_2\text{NH}]\text{-Asp-Ile-Trp}$ (5). The peptide synthesis, cleavage from the resin, and deprotection were performed as described in the general procedure. The crude peptide was purified by reversed-phase HPLC to afford 33 mg of the title compound: HPLC t_R = 14.6 min (>96%); ESMS (m/z)⁺ calcd 910.1, found 910.4 (M).

Preparation of Ac- α Dip-Leu-Asp- $\Psi[\text{CH}_2\text{NH}]\text{-Ile-Trp}$ (6). Preparation of N^{α} -*t*-Boc-Asp(ObzI)- CH_2OH . To a solution of N^{α} -*t*-Boc-Asp(ObzI) (6.3 g, 20 mmol) in dry THF (20 mL) at 0 °C under N_2 was added 1 M $\text{BH}_3\text{-THF}$ (40 mL, 40 mmol) dropwise over a period of 2 h. The solution was stirred for an additional 2 h at 0 °C, and 20 mL of HOAc was added. The reaction mixture was evaporated under reduced pressure, dissolved in EtOAc (100 mL), washed with 10% aqueous NaHCO_3 , water, 1 N HCl, and brine (2 \times 50 mL, each), dried with MgSO_4 , filtered, and concentrated under reduced pressure to an oil (5.5 g, 90%): $^1\text{H-NMR}$ (CDCl_3) δ 1.45 (s, 9H), 2.15 (d, 2H), 2.20 (br, 1H), 3.65 (d, 2H), 4.01 (m, 1H), 5.12 (s, 2H), 5.33 (d, 1H), 7.45 (m, 5H); CIMS (m/z)⁺ calcd 309.4, found 310 (M), 210 (M - Boc).

Preparation of N^{α} -*t*-Boc-Asp(ObzI)-CHO. To a solution of N^{α} -*t*-Boc-Asp(ObzI)- CH_2OH (2.0 g, 9.7 mmol) in DCM was added pyridinium dichromate (5.7 g, 15.0 mmol). The solution was allowed to stir at room temperature overnight. The reaction mixture was filtered through a Celite pad, and the filtrate was evaporated to dryness under reduced pressure to an oil (1.5 g, 75%). This oil was used without further purification.

Preparation of Ac- α Dip-Leu-Asp- $\Psi[\text{CH}_2\text{NH}]\text{-Ile-Trp}$ (6). The peptide synthesis, cleavage from the resin, and deprotection were performed as described in the general procedure. The crude peptide was purified by reversed-phase HPLC to afford 43 mg of the title compound: HPLC t_R = 15.9 min (>97%); ESMS (m/z)⁺ calcd 910.1, found 910.5 (M).

Preparation of Ac- α Dip-Leu-Asp- $\Psi[\text{CH}_2\text{NH}]\text{-Ile-Trp}$ (7). Preparation of N^{α} -Cbz-Ile- $\Psi[\text{CH}_2\text{NH}]\text{-Ile-OMe}$. N^{α} -Cbz-Ile-CHO was prepared in two steps from N^{α} -Cbz-Ile-CHO as described for N^{α} -*t*-Boc- α Dip-CHO (8.3 g, 64%). N^{α} -Cbz-Ile-CHO was dissolved in dry MeOH (250 mL) and treated with Ile-OMe-HCl (4.8 g, 33.4 mmol) followed by NaBH_3CN (2.8 g, 44.3 mmol) and acetic acid (2.0 mL, 33.3 mmol). The reaction mixture was allowed to stir overnight and concentrated under reduced pressure to dryness. The residue was dissolved in EtOAc (100 mL), washed with saturated aqueous NaHCO_3 and brine (2 \times 50 mL, each), dried with Na_2SO_4 , filtered, and concentrated under reduced pressure to an oil which crystallized upon standing (9.35 g, 74%): $^1\text{H-NMR}$ (CDCl_3) δ 0.88 (m, 12H), 1.45 (m, 7H), 2.42 (m, 1H), 2.78 (m, 1H), 3.02 (d, 1H), 3.59 (m, 1H), 3.69 (s, 3H), 4.88 (m, 1H), 5.10 (s, 2H), 7.35 (s, 5H); CIMS (m/z)⁺ calcd 378.4, found 379 (M + H).

Preparation of N^{α} -Cbz-Ile- $\Psi[\text{CH}_2\text{NH}]\text{-Ile}$. To a solution of N^{α} -Cbz-Ile- $\Psi[\text{CH}_2\text{NH}]\text{-Ile-OMe}$ (4.35 g, 11.5 mmol) in *p*-dioxane (45 mL) was added 1 M aqueous LiOH (12.5 mL, 12.5 mmol). The reaction mixture was stirred at room temperature for 4 days. The solvent was removed under reduced pressure, and the residue was dissolved in water (10 mL). The resulting solution was treated with 2 N HCl (23 mL). The precipitate which formed was collected and dried (3.1 g, 74%): $^1\text{H-NMR}$ ($\text{DMSO}-d_6$) δ 1.35 (m, 6H), 2.52 (m, 1H), 2.78 (m, 1H), 2.99 (d, 2H), 5.02 (s, 1H), 7.22 (d, 1H), 7.35 (s, 5H); CIMS (m/z)⁺ calcd 364.4, found 365 (M + H).

Preparation of N^{α} -Fmoc-Ile- $\Psi[\text{CH}_2\text{NH}]\text{-Ile}$. N^{α} -Cbz-Ile- $\Psi[\text{CH}_2\text{NH}]\text{-Ile}$ was dissolved in MeOH (50 mL) and hydrogenated in the presence of 20% Pd/C (0.30 g) for 2 h. The reaction mixture was filtered, and the solvent was concentrated under reduced pressure to a white powder (1.8 g) which was suspended in a mixture of water-*p*-dioxane (1:1, 70 mL). The solution was treated with triethylamine (2.7 mL, 19.5 mmol) followed by Fmoc-OSu (2.6 g, 7.7 mmol). The reaction mixture was stirred at room temperature overnight, and treated with an aqueous solution of KHSO_4 (2.7 g, 19.5 mmol in 100 mL). The precipitate was collected, triturated with

EtOAc :hexane (1:4), and dried under reduced pressure to a white solid (2.0 g, 51%); CIMS (m/z)⁺ calcd 452.1, found 453 (M + H).

Preparation of $\text{Ac}\text{-}\text{Dip}\text{-Leu}\text{-Asp}\text{-Ile}\text{-}\Psi[\text{CH}_2\text{NH}]\text{-Ile}\text{-Trp}$ (7). The peptide synthesis, cleavage from the resin, and deprotection were performed as described in the general procedure. The crude peptide was purified by reversed-phase HPLC to afford 190 mg of the title compound; HPLC $t_R = 14.5$ min (>98%); FABMS (m/z)⁺ calcd 910.1, found 910.7 (M).

Preparation of $\text{Ac}\text{-}\text{Dip}\text{-Leu}\text{-Asp}\text{-Ile}\text{-Ile}\text{-}\Psi[\text{CH}_2\text{NH}]\text{-Trp}$ (8). Preparation of $\text{N}^a\text{-}t\text{-Boc}\text{-Ile}\text{-N}(\text{CH}_3)\text{OCH}_3$. To a solution of $\text{N}^a\text{-}t\text{-Boc}\text{-Ile}$ (10 g, 43.2 mmol) in DMF (20 mL) were added $\text{HCl}\text{-HN}(\text{CH}_3)\text{OCH}_3$ (4.4 g, 45.1 mmol) and DIEA (15.7 mL, 90.1 mmol) followed by BOP reagent (9.1 g, 43.2 mmol). The reaction mixture was stirred for 2 h. The reaction mixture was then concentrated under reduced pressure to dryness. The residue was taken up with EtOAc (100 mL), washed with saturated aqueous Na_2CO_3 , water, and 1 M aqueous KHSO_4 (2 \times 50 mL, each), dried with MgSO_4 , and concentrated under reduced pressure to give a pale yellow oil (10.1 g, 91%); $^1\text{H-NMR}$ (CDCl_3) δ 0.95 (m, 6H), 1.38 (s, 9H), 1.50 (m, 2H), 1.74 (m, 1H), 3.21 (s, 3H), 3.80 (s, 3H), 4.80 (m, 1H), 5.33 (d, 1H); CIMS (m/z)⁺ calcd 274.1, found 274 (M).

Preparation of $\text{N}^a\text{-}t\text{-Boc}\text{-Ile}\text{-CHO}$. To a solution of $\text{N}^a\text{-}t\text{-Boc}\text{-Ile}\text{-N}(\text{CH}_3)\text{OCH}_3$ (10.0 g, 38.9 mmol) in dry THF (200 mL) at 0 °C was added, in portions, lithium aluminum hydride (1.7 g, 44.8 mmol). The reaction was stirred for 30 min at 0 °C and quenched by the addition of 1 M aqueous KHSO_4 (100 mL). The organic phase was separated and the aqueous phase extracted with EtOAc (100 mL). The combined organic phases was washed with brine (1 \times 50 mL), dried with MgSO_4 , filtered, and concentrated under reduced pressure to a colorless oil (6.6 g 87%); $^1\text{H-NMR}$ (CDCl_3) δ 0.96 (m, 6H), 1.36 (s, 9H), 1.38–1.84 (m, 3H), 4.38 (m, 1H), 5.38 (d, 1H), 9.60 (s, 1H); CIMS (m/z)⁺ calcd 215.3, found 216 (M + H).

Preparation of $\text{N}^a\text{-}t\text{-Boc}\text{-Ile}\text{-}\Psi[\text{CH}_2\text{NH}]\text{-Trp}\text{-PAM-Resin}$. $\text{N}^a\text{-}t\text{-Boc}\text{-Trp}\text{-PAM}$ resin (1.0 mmol total) was treated with 50% TFA in DCM (20 mL) for 30 min at room temperature; the resin was washed successively with DCM (3 \times 20 mL), 10% DIEA in DCM (20 mL), DMF (3 \times 20 mL), and 5% HOAc in DMF (2 \times 20 mL). $\text{N}^a\text{-}t\text{-Boc}\text{-Ile}\text{-CHO}$ (2.5 mmol) was added followed by 1% acetic acid in DMF (20 mL) and NaBH_3CN (2.5 mmol). The mixture was shaken at room temperature for 3 h. The resin was washed with DMF, MeOH , and DCM (3 \times 20 mL, each) and dried under reduced pressure.

Preparation of $\text{Ac}\text{-}\text{Dip}\text{-Leu}\text{-Asp}\text{-Ile}\text{-Ile}\text{-}\Psi[\text{CH}_2\text{NH}]\text{-Trp}$ (8). The peptide synthesis, cleavage from the resin, and deprotection were performed as described in the general procedure. The crude peptide was purified by reversed-phase HPLC to afford 30 mg of the title compound; HPLC $t_R = 14.5$ min (>98%); FABMS (m/z)⁺ calcd 910.1, found 910.7 (M).

Preparation of $\text{Ac}\text{-}[\text{NMe}]\text{Dip}\text{-Leu}\text{-Asp}\text{-Ile}\text{-Ile}\text{-Trp}$ (9). Preparation of $\text{N}^a\text{-}4,4'\text{-Dimethoxyphenylmethyl(Dod)\text{-Dip}\text{-Leu}\text{-Asp(OBzI)\text{-Ile}\text{-Ile}\text{-Trp}\text{-PAM Resin}}$. $\text{N}^a\text{-}t\text{-Boc}\text{-Dip}\text{-Leu}\text{-Asp(OBzI)\text{-Ile}\text{-Ile}\text{-Trp}\text{-PAM}$ resin (0.5 mmol) was prepared as described in the general procedure. $\text{N}^a\text{-}t\text{-Boc}\text{-Dip}\text{-Leu}\text{-Asp(OBzI)\text{-Ile}\text{-Ile}\text{-Trp}\text{-PAM}$ resin (0.5 mmol) was treated with 50% TFA/DCM for 30 min in a manual shaker and washed with DCM (3 \times 20 mL), 10% DIEA/DCM (20 mL), and DCM (2 \times 20 mL). Dod-Cl (0.20 g, 0.76 mmol) in DCM (20 mL) was added followed by DIEA (0.5 mL). The reaction was allowed to proceed for 1 h. The resin was drained washed with DCM and DMF (3 \times 20 mL, each), and dried under reduced pressure.

Preparation of $\text{H}\text{-}[\text{NMe}]\text{Dip}\text{-Leu}\text{-Asp(OBzI)\text{-Ile}\text{-Ile}\text{-Trp}\text{-PAM Resin}}$. The formaldehyde in DMF solution was prepared as follows: To a 38% aqueous formaldehyde solution (20 mL) was added to DMF (180 mL) followed by MgSO_4 (50 g). The solution was stirred for 1 h under N_2 and filtered. The filtrate (20 mL) was added to $\text{N}^a\text{-Dip}\text{-Dip}\text{-Leu}\text{-Asp(OBzI)\text{-Ile}\text{-Ile}\text{-Trp}\text{-PAM}$ resin followed by HOAc (0.30 mL) and 1 M NaBH_3CN in DMF (1.25 mL, 1.25 mmol). The mixture was shaken for 30 min and the procedure repeated. The resin was then treated with 50%TFA/DCM (2 \times 20 mL, 20 min each), washed in turn with DCM, 10% DIEA/DCM, and DMF (3 \times 20 mL, each), and dried under reduced pressure.

Preparation of $\text{Ac}\text{-}[\text{NMe}]\text{Dip}\text{-Leu}\text{-Asp}\text{-Ile}\text{-Ile}\text{-Trp}$ (9). $\text{H}\text{-}[\text{NMe}]\text{Dip}\text{-Leu}\text{-Asp(OBzI)\text{-Ile}\text{-Ile}\text{-Trp}}$ was cleaved from the resin and deprotected using anhydrous HF:anisole (9:1, 0 °C, 60 min). The crude peptide was purified by reversed-phase HPLC and lyophilized. The purified peptide was dissolved in 90% HOAc (20 mL) and treated with acetic anhydride (2 mL) for 2 h. Evaporation followed by lyophilization afforded 40 mg of the title compound; HPLC $t_R = 18.5$ min (97%); ESMS (m/z)⁺ calcd 938.1, found 937.6 (M).

Preparation of $\text{Ac}\text{-}\text{Dip}\text{-}[\text{NMe}]\text{Leu}\text{-Asp}\text{-Ile}\text{-Ile}\text{-Trp}$ (10). The peptide synthesis, cleavage from the resin, and deprotection were performed as described in the general procedure. $\text{N}^a\text{-}t\text{-Boc}\text{-}[\text{NMe}]\text{Leu}$ was obtained from commercial sources. The crude peptide was purified by reversed-phase HPLC to afford 18.0 mg of the title compound; HPLC $t_R = 17.5$ min (>98%); ESMS (m/z)⁺ calcd 938.1, found 939.1 (M + H).

Preparation of $\text{Ac}\text{-}\text{Dip}\text{-Leu}\text{-}[\text{NMe}]\text{Asp}\text{-Ile}\text{-Ile}\text{-Trp}$ (11). Preparation of $\text{N}^a\text{-Fmoc}\text{-}[\text{NMe}]\text{Asp(OBzI)}$. To a suspension of $\text{N}^a\text{-Fmoc}\text{-Asp(OBzI)}$ (3.0 g, 9.3 mmol) and paraformaldehyde (2.0 g) in toluene (100 mL) was added *p*-toluenesulfonic acid (0.2 g). The mixture was refluxed with azeotropic water removal for 30 min. The reaction mixture was then cooled to room temperature, washed with saturated aqueous NaHCO_3 and brine (2 \times 50 mL, each), dried with MgSO_4 , filtered, and concentrated under reduced pressure (oil, 2.8 g) which was then treated with a mixture of CHCl_3 (50 mL), TFA (40 mL), and Et_3SiH (4.3 mL, 27.0 mmol) at room temperature for 40 h. The reaction mixture was evaporated under reduced pressure to dryness. The residue was dissolved in EtOAc (50 mL), washed with saturated aqueous NaHCO_3 , water, 1 N HCl, and brine (2 \times 50 mL, each), filtered, dried with MgSO_4 , and concentrated under reduced pressure to a foam. Crystallization from EtOAc /hexane yielded a white powder (2.5 g, 80%); $^1\text{H-NMR}$ (CDCl_3) δ 2.85 (m, 1H), 2.90 (s, 3H), 3.11 (m, 2H), 4.25 (m, 2H), 5.12 (m, 2H), 7.25 (m, 7H), 7.55 (m, 3H), 7.78 (m, 3H) [In the $^1\text{H-NMR}$ of this compound a doubling of the resonances was observed, presumably due to rotational isomerization about the urethane bond. In this case the chemical shift of the major isomer is reported (probably the *trans* conformer), but the total integration of both resonances is reported.] FABMS (m/z)⁺ calcd 459.5, found 459.1 (M).

Preparation of $\text{Ac}\text{-}\text{Dip}\text{-Leu}\text{-}[\text{NMe}]\text{Asp}\text{-Ile}\text{-Ile}\text{-Trp}$ (11). The peptide synthesis, cleavage from the resin, and deprotection were performed as described in the general procedure. The crude peptide was purified by reversed-phase HPLC to afford 25.8 mg of the title compound; HPLC $t_R = 15.0$ min (>99%); ESMS (m/z)⁺ calcd 938.1, found 939.4 (M + H), 960.1 (M + Na).

Preparation of $\text{Ac}\text{-}\text{Dip}\text{-Leu}\text{-Asp}\text{-}[\text{NMe}]\text{Ile}\text{-Ile}\text{-Trp}$ (12). The peptide synthesis, cleavage from the resin, and deprotection were performed as described in the general procedure. $\text{N}^a\text{-}t\text{-Boc}\text{-}[\text{NMe}]\text{Ile}$ was obtained from commercial sources. The crude peptide was purified by reversed-phase HPLC to afford 58.5 mg of the title compound; HPLC $t_R = 18.5$ min (97%); ESMS (m/z)⁺ calcd 938.1, found 938.1 (M), 960.7 (M + Na).

Preparation of $\text{Ac}\text{-}\text{Dip}\text{-Leu}\text{-Asp}\text{-}[\text{NMe}]\text{Ile}\text{-Ile}\text{-Trp}$ (13). Preparation of $\text{N}^a\text{-Fmoc}\text{-Ile}\text{-COCl}$. To a suspension of $\text{N}^a\text{-Fmoc}\text{-Ile}$ (10.0 g, 28.3 mmol) in DCM (100 mL) was added oxalyl chloride (2.9 mL, 33.0 mmol) dropwise at 0 °C. The reaction mixture was stirred for 1 h at 0 °C and warmed to room temperature. The reaction mixture was stirred at room temperature for an additional 2 h and evaporated under reduced pressure to an oil (8.5 g, 81%); $^1\text{H-NMR}$ (CDCl_3) δ 0.85 (t, 3H), 1.05 (d, 3H), 1.18 (m, 1H), 1.45 (m, 1H), 2.12 (m, 2H), 4.25 (t, 1H), 4.50 (m, 2H), 5.25 (d, 1H), 7.25 (t, 2H), 7.38 (t, 2H), 7.55 (m, 2H), 7.74 (d, 2H) [In the $^1\text{H-NMR}$ for this compound a doubling of the resonances was observed, presumably due to rotational isomerization about the urethane bond. In this case the chemical shift of the major isomer is reported (probably the *trans* conformer), but the total integration of both resonances is reported.] CIMS (m/z)⁺ calcd 370.2, found 369 (M + H).

Preparation of $\text{N}^a\text{-Fmoc}\text{-Ile}\text{-}[\text{NMe}]\text{Ile}\text{-Trp}\text{-PAM Resin}$. $\text{N}^a\text{-}t\text{-Boc}\text{-}[\text{NMe}]\text{Ile}\text{-Trp}\text{-PAM}$ resin (0.5 mmol) was prepared as described in the general procedure. $\text{N}^a\text{-}t\text{-Boc}\text{-}[\text{NMe}]\text{Ile}$ was obtained from commercial sources. $\text{N}^a\text{-}t\text{-Boc}\text{-}[\text{NMe}]\text{Ile}\text{-Trp}\text{-PAM}$

PAM resin was treated with 50% TFA/DCM (20 mL) for 30 min and washed with DCM (3 × 20 mL), 10% DIEA/DCM (20 mL), and DCM (3 × 20 mL). N^{α} -Fmoc-Ile-COCl (0.6 g, 1.6 mmol) in DCM (20 mL) was added followed by DIEA (2.7 mL, 1.55 mmol). The reaction mixture was shaken for 2 h, and the procedure was repeated. The peptide resin was then washed with DCM (3 × 20 mL) and dried under reduced pressure.

Preparation of Ac- α Dip-Leu-Asp-Ile-[NMe]Ile-Trp (13). The peptide synthesis, cleavage from the resin, and deprotection were performed as described in the general procedure. The crude peptide was purified by reversed-phase HPLC to afford 70.1 mg of the title compound: HPLC t_R = 17.3 min (98%); ESMS (m/z)⁺ calcd 938.1, found 939.1 (M + H).

Preparation of Ac- α Dip-Leu-Asp-Ile-Ile-[NMe]Trp (14). Preparation of N^{α} -DOD-Trp-PAM Resin. N^{α} -*t*-Boc-Trp-PAM resin (0.5 mmol) was treated with 50% TFA/DCM for 30 min in a manual shaker and washed with DCM (3 × 20 mL), 10% DIEA/DCM (20 mL), and DCM (2 × 20 mL). DOD-Cl (0.20 g, 0.76 mmol) in DCM (20 mL) was added followed by DIEA (0.5 mL). The reaction was allowed to proceed for 1 h. The resin was drained, washed with DCM and DMF (3 × 20 mL, each), and dried under reduced pressure.

Preparation of H-[NMe]Trp-PAM Resin. The formaldehyde in DMF solution was prepared as follows: To a 38% aqueous formaldehyde solution (20 mL) was added DMF (180 mL) followed by MgSO₄ (50 g). The solution was stirred for 1 h and filtered. The filtrate (20 mL) was added to N^{α} -DOD-Trp-PAM resin followed by HOAc (0.30 mL) and 1 M NaBH₃CN in DMF (1.25 mL, 1.25 mmol). The mixture was shaken for 30 min and the procedure repeated. The resin was then treated with 50% TFA/DCM (2 × 20 mL, 20 min each), washed in turn with DCM, 10% DIEA/DCM, and DMF (3 × 20 mL, each), and dried under reduced pressure.

Preparation of Ac- α Dip-Leu-Asp-Ile-Ile-[NMe]Trp (14). The peptide synthesis was performed as described in the general procedure. After the coupling of N^{α} -*t*-Boc- α Dip, the peptide resin was treated with 50% TFA/DCM (30 min), and the peptide was deprotected and cleaved from the resin using anhydrous HF:anisole (9:1, 0 °C, 60 min). The crude peptide was purified by reversed-phase HPLC and lyophilized. The purified peptide was dissolved in 90% acetic acid (20 mL) and treated with acetic anhydride (2 mL) for 2 h. Evaporation followed by lyophilization afforded 40 mg of the title compound: HPLC t_R = 16.7 min (97%); ESMS (m/z)⁺ calcd 938.1, found 937.6 (M).

Preparation of Ac- α Bhg-Leu-Asp-Ile-[NMe]Ile-Trp (15). The peptide synthesis, cleavage from the resin, and deprotection were performed as described for Ac- α Dip-Leu-Asp-Ile-[NMe]Ile-Trp (compound 13). The crude peptide was purified by reversed-phase HPLC to afford 530 mg of the title compound: HPLC t_R = 18.0 min (>97%); ESMS (m/z)⁺ calcd 964.1, found 963.4 (M).

Endothelin Receptor Binding Assay Protocol. The receptor binding assay protocols using rabbit renal vascular smooth muscle cells (ET_A), rat cerebellar membranes (ET_B), or the corresponding cloned human ET_A and ET_B receptors have been previously described.²⁹

In Vitro Contractility Studies. The experimental protocols using vascular rings of rat femoral artery (ET_A) or rabbit pulmonary artery (ET_B) have been previously described.²⁹

Caco-2 Cell Transport and Stability in Rat Intestinal Perfusate Experiments. These studies were performed as previously described.³⁴

Conscious Rat Duration of Action Study with PD 156252. Nonfasted rats (350–500 g) were anesthetized with methoxyflurane by inhalation and instrumented with a jugular cannula (PE50) for iv administration of test agents and with a carotid artery cannula (PE50) for arterial blood pressure measurements. Rats were attached to a swivel for freedom of movement, and food and water were available ad libidum. Prior to the experiment, the animals were allowed to recover from the anesthesia for 60 min. Following recovery the rats were ganglionically blocked with mecamylamine-HCl (1.25 mg/kg, iv) 20 min prior to the ET-1 challenge (0.30 nM/kg, iv).

bolus). Compound 15 was administered at a dose of 10 mg/kg (iv, bolus) 5 and 30 min prior to the ET-1 challenge.

Nuclear Magnetic Resonance Studies. ¹H-NMR spectra were recorded on a Bruker AMX 500 spectrometer using samples typically 5–10 mM dissolved in deuterated solvents obtained from Cambridge Isotope Laboratories. Two-dimensional total correlation spectroscopy (TOCSY),⁴⁴ double-quantum-filtered correlation spectroscopy (dqc-COSY),⁴⁵ rotating frame nuclear Overhauser spectroscopy (ROESY),^{46,47} and nuclear Overhauser spectroscopy (NOESY)⁴⁸ were acquired as 1024 × 512 matrices and were processed using UXNMR (Bruker Instruments). Quadrature detection in the t_1 dimension was achieved by the time proportional phase incrementation (TPPI)⁴⁹ method in 2D spectra. Prior to zero-filling to 1K in the second dimension and Fourier transformation, \cos^2 weighting functions were applied to the time domain data in both dimensions. Finally, the baselines in the 2D time domain matrices were flattened using a polynomial fitting routine. NOE data were converted to distance constraints as previously described.⁵⁰ NOESY cross-peaks for which volume buildup curves (30–400 ms) suggested contributions from spin diffusion were excluded from the analysis. Coupling constants were measured directly from resolution-enhanced 1D spectra and were used as converted to dihedral constraints where warranted. Amide temperature coefficients were measured relative to an internal reference [3-(trimethylsilyl)propionic acid-*d*₄ sodium salt (TSP) for aqueous samples, the residual solvent resonance in organic solvents] for at least three different temperatures. Structures were generated using the distance geometry/simulated annealing program DGII (Biosym Technologies) followed by constrained energy minimization using a previously described protocol.⁵⁰

Secondary shifts were calculated by subtracting the random coil chemical shift from the observed chemical shift, and all observed chemical shifts were referenced directly or indirectly to TSP protons at 0.0 ppm.⁵¹ Carbon-13 random coil chemical shifts for natural amino acids were obtained from the appropriate literature references for peptides dissolved in D₂O⁵¹ and DMSO.⁵² To correct the DMSO solution random coil chemical shifts for referencing relative to TSP protons, 3.34 ppm was added to the reported values. For unnatural residues, random coil shifts were measured in the peptides Gly-Gly-Xxx-Gly-Gly, where Xxx = DBhg and [NMe]Ile as previously described.⁵¹ The random coil chemical shifts used to calculate secondary shifts are provided in the Supporting Information. For the disodium salt peptides, 1.5 ppm was added to the random coil chemical shift of the α carbon of Asp¹⁸ to compensate for differences in ionization state from the literature values. This correction factor was derived from the reported shifts for Asp carbons in the neutral and anionic forms of Asp-containing peptides in D₂O.⁵² For Ile¹⁹ in compound 15, 2.4 ppm was subtracted from the random coil chemical shift of the Ile α carbon to compensate for its attachment to a tertiary amide group.⁵³ This correction factor was derived from the reported shifts for Ile in the peptides Gly-Gly-Ile-Ala-Gly-Gly and Gly-Gly-Ile-Pro-Gly-Gly.⁵²

Acknowledgment. The authors would like to thank Dana DeJohn Joseph Loo, Tracy Stevenson, and Brian Tobias for analytical and spectral data; Michael Flynn and Kathleen Welch for pharmacological data; Vlad Beylin, Huaiyu Chen, and Om Goel for the preparation of α Dip and α Bhg; and James Kaltenbronn and Bill Reisdorph for the preparation of protected intermediates.

Supporting Information Available: Tables containing selected ¹H-NMR data for compounds 3 and 15 and the random coil chemical shifts used to calculate secondary shifts and figures illustrating the secondary Ca/Ha chemical shifts of compounds 3 and 15 and the titration of compound 15 (7 pages). Ordering information is given on any current masthead page.

References

- Hickey, K. A.; Rubanyi, G.; Paul, R. J.; Highsmith, R. F. Characterization of a coronary vasoconstrictor produced by endothelial cells in culture. *Am. J. Physiol.* 1985, 248, C550-C556.
- Yanagisawa, M.; Kurihara, H.; Kimura, S.; Tomobe, Y.; Kobayashi, M.; Mitsui, Y.; Goto, K.; Masaki, T. A novel potent vasoconstrictor peptide produced by vascular endothelial cells. *Nature (London)* 1988, 332, 411-415.
- Yanagisawa, M.; Inoue, A.; Ishikawa, T.; Kasuya, T.; Kimura, S.; Kumagai, S.; Nakajima, K.; Watanabe, T. K.; Sakabibara, S.; Goto, K.; Masaki, T. Primary structure, synthesis, and biological activity of rat endothelin, an endothelium-derived vasoconstrictor peptide. *Proc. Natl. Acad. Sci. U.S.A.* 1989, 86, 6964-6967.
- Inoue, A.; Yanagisawa, M.; Kimura, S.; Kasuya, Y.; Miyauchi, T.; Goto, K.; Masaki, T. The human endothelin family: Three structurally and pharmacologically distinct isopeptides predicted by three separate genes. *Proc. Natl. Acad. Sci. U.S.A.* 1989, 86, 2863-2867.
- Saida, K.; Mitsui, Y.; Ishida, N. A novel peptide, vasoactive intestinal contractor, of a new (endothelin) peptide family. Molecular cloning, expression and biological activity. *J. Biol. Chem.* 1989, 264, 14613-14616.
- Kloog, T.; Ambar, I.; Sokolovsky, M.; Kochva, E.; Wolberg, Z.; Bdolah, A. Sarafotoxin, a novel vasoconstrictor peptide: Phosphoinositide hydrolysis in rat heart and brain. *Science* 1988, 242, 268-270.
- Bdolah, A.; Wolberg, Z.; Fleminger, G.; Kochva, E. SRTX-d, a new native peptide of the endothelin/sarafotoxin family. *FEBS Lett.* 1989, 251, 1-3.
- Becker, A.; Dowdle, E. B.; Hechler, U.; Kauser, K.; Donner, P.; Schleuning, W. D. Birotoxin, a novel member of the endothelin/sarafotoxin peptide family, from the venom of the burrowing asp, *Atractaspis bibroni*. *FEBS Lett.* 1993, 315, 100-103.
- Doherty, A. M. Endothelin: A new challenge. *J. Med. Chem.* 1992, 35, 1493-1508.
- Huggins, J. P.; Pelton, J. T.; Miller, R. C. The structure and specificity of endothelin receptors: Their importance in physiology and medicine. *Pharmacol. Ther.* 1993, 59, 55-123.
- Cheng, X. M.; Nikam, S. S.; Doherty, A. M. Development of agents to modulate the effects of endothelin. *Cur. Med. Chem.* 1995, 1, 271-312.
- Cody, W. L.; Doherty, A. M. Development of agents to modulate the effects of endothelin. *Biopolymers (Pept. Sci.)* 1995, 37, 89-104.
- Arai, H.; Hori, T.; Aramori, I.; Ohkubo, H.; Nakanishi, S. Cloning and expression of a cDNA encoding an endothelin receptor. *Nature (London)* 1990, 348, 730-732.
- Sakurai, T.; Yanagisawa, M.; Takuwa, Y.; Miyazaki, H.; Kimura, S.; Goto, K.; Masaki, T. Cloning of a cDNA encoding a nonisopeptide-selective subtype of the endothelin receptor. *Nature (London)* 1990, 348, 732-735.
- Sakamoto, A.; Yanagisawa, M.; Sakurai, T.; Takuwa, Y.; Yanagisawa, H.; Masaki, T. Cloning and functional expression of human cDNA for ET_A endothelin receptor. *Biochem. Biophys. Res. Commun.* 1991, 178, 656-663.
- Hosoda, K.; Nakao, K.; Arai, H.; Suga, S.; Ogawa, Y.; Mukoyama, M.; Shirakami, G.; Saito, T.; Nakanishi, S.; Imura, H. Cloning and expression of human endothelin-1 receptor cDNA. *FEBS Lett.* 1991, 287, 23-26.
- Williams, D. L.; Jones, K. L.; Pettibone, D. L.; Lis, E. V.; Clineschmidt, B. V. Sarafotoxin S6c: An agonist which distinguishes between endothelin receptor subtypes. *Biochem. Biophys. Res. Commun.* 1991, 175, 556-561.
- Takayanagi, R.; Kitazumi, K.; Takasaki, C.; Ohnaka, K.; Aimoto, S.; Tasaka, K.; Ohashi, M.; Nawata, H. Presence of non-selective type of endothelin receptor on vascular endothelium and its linkage to vasodilation. *FEBS Lett.* 1991, 282, 103-106.
- Saeki, T.; Ihara, M.; Fukuroda, T.; Yamagishi, M.; Yano, M. [Ala^{1,3,11,15}]Endothelin-1 analogs with ET_B agonist activity. *Biochem. Biophys. Res. Commun.* 1991, 179, 286-292.
- Panek, R. L.; Major, T. C.; Hingorani, G. P.; Doherty, A. M.; Taylor, D. G.; Rapundalo, S. T. Endothelin and structurally related analogs distinguish between receptor subtypes. *Biochem. Biophys. Res. Commun.* 1992, 183, 566-571.
- Sudjarwo, S. A.; Hori, M.; Takai, M.; Urade, Y.; Okada, T.; Karaki, H. A novel type of endothelin B receptor mediating contraction in swine pulmonary vein. *Life Sci.* 1993, 53, 431-437.
- Warner, T. D.; Alcock, G. H.; Corder, R.; Vane, J. R. Use of the endothelin antagonists BQ-123 and PD 142893 to reveal three endothelin receptors mediating smooth muscle contraction and the release of EDRF. *Br. J. Pharmacol.* 1993, 110, 777-782.
- Reynolds, E. E.; Hwang, O.; Flynn, M. A.; Welch, K. M.; Cody, W. L.; Steinbaugh, B.; He, J. X.; Chung, F. Z.; Doherty, A. M. Pharmacological differences between rat and human endothelin B receptors. *Biochem. Biophys. Res. Commun.* 1995, 209, 506-512.

- Doherty, A. M.; Cody, W. L.; Leitz, N. L.; DePue, P. L.; Taylor, M. D.; Rapundalo, S. T.; Hingorani, G. P.; Major, T. C.; Panek, R. L.; Taylor, D. G. Structure-activity studies of the C-terminal region of the endothelins and the sarafotoxins. *J. Cardiovasc. Pharmacol.* 1991, 17 (Suppl. 7), S59-S61.
- Cody, W. L.; Doherty, A. M.; He, J. X.; DePue, P. L.; Rapundalo, S. T.; Hingorani, G. A.; Major, T. C.; Panek, R. L.; Dudley, D. T.; Haleen, S. J.; LaDouceur, D.; Hill, K. E.; Flynn, M. A.; Reynolds, E. E. Design of a functional hexapeptide antagonist of endothelin. *J. Med. Chem.* 1992, 35, 3301-3303.
- Doherty, A. M.; Cody, W. L.; He, J. X.; DePue, P. L.; Leonard, D. M.; Dunbar, J. B.; Hill, K. E.; Flynn, M. A.; Reynolds, E. E. Design of C-terminal peptide antagonists of endothelin: Structure-activity relationships of $ET-1(16-21,D-His^{18})$. *Bioorg. Med. Chem. Lett.* 1993, 3, 497-502.
- Doherty, A. M.; Cody, W. L.; DePue, P. L.; He, J. X.; Waite, L. A.; Leonard, D. M.; Leitz, N. L.; Dudley, D. T.; Rapundalo, S. T.; Hingorani, G. P.; Haleen, S. J.; LaDouceur, D. M.; Hill, K. E.; Flynn, M. A.; Reynolds, E. E. Structure-activity relationships of C-terminal endothelin hexapeptide antagonists. *J. Med. Chem.* 1993, 36, 2585-2594.
- Cody, W. L.; Doherty, A. M.; He, J. X.; DePue, P. L.; Waite, L. A.; Haleen, S. J.; LaDouceur, D. M.; Flynn, M. A.; Welch, K. M.; Reynolds, E. E. Endothelin antagonists: The rational design of combined and ET_B receptor subtype selective antagonists. In *Peptides, Chemistry, Structure and Biology: Proceedings of the Thirteenth American Peptide Symposium*; Hodges, R. S., Smith, J. A., Eds.; ESCOM Science: Leiden, The Netherlands, 1994; pp 598-600.
- Cody, W. L.; Doherty, A. M.; He, J. X.; DePue, P. L.; Waite, L. A.; Leonard, D. M.; Seifler, A. M.; Kaltenbronn, J. S.; Haleen, S. J.; Walker, D. M.; Flynn, M. A.; Welch, K. M.; Reynolds, E. E.; Doherty, A. M. Structure-activity relationships of the potent combined endothelin-A/endothelin-B receptor antagonist $Ac-Dip^{16}-Leu-Asp-Ile-Ile-Trp^{21}$: Development of endothelin-B receptor selective antagonists. *J. Med. Chem.* 1995, 38, 2809-2819.
- Cody, W. L.; Doherty, A. M.; He, J. X.; Topliss, J. G.; Haleen, S. J.; LaDouceur, D.; Flynn, M. A.; Hill, K. E.; Reynolds, E. E. Structure-activity relationships in the C-terminus of endothelin-1 (ET-1): The discovery of potent antagonists. In *Peptides 1992: Proceedings of the Twenty-Second European American Peptide Symposium*; Schneider, C. H., Eberle, A. N., Eds.; ESCOM Science: Leiden, The Netherlands, 1993; pp 687-688.
- Cody, W. L.; Doherty, A. M.; He, J. X.; DePue, P. L.; Waite, L. A.; Topliss, J. G.; Haleen, S. J.; LaDouceur, D.; Flynn, M. A.; Hill, K. E.; Reynolds, E. E. The rational design of a highly potent combined ET_A and ET_B receptor antagonist (PD 145065) and related analogues. *Med. Chem. Res.* 1993, 3, 154-162.
- Doherty, A. M.; Cody, W. L.; He, J. X.; DePue, P. L.; Cheng, X. M.; Welch, K. M.; Flynn, M. A.; Reynolds, E. E.; LaDouceur, D. M.; Davis, L. S.; Keiser, J. A.; Haleen, S. J. In vitro and in vivo studies with a series of hexapeptide endothelin antagonists. *J. Cardiovasc. Pharmacol.* 1993, 22 (Suppl. 8), S98-S102.
- Cody, W. L.; He, J. X.; Doherty, A. M.; DePue, P. L.; Kaltenbronn, J. S.; Reisdorph, B. R.; Walker, D. M.; Welch, K. M.; Haleen, S. J.; Reynolds, E. E.; Tse, E.; Reyner, E. L.; Stewart, B. H. The design of potent hexapeptide endothelin antagonists stable to proteolysis. In *Peptides 1994: Proceedings of the Twenty-Third European Peptide Symposium*; Maia, H. L. S., Ed.; ESCOM Science: Leiden, The Netherlands, 1993; pp 38-39.
- Stewart, B. H.; Reyner, E. L.; Tse, E.; Hayes, R. N.; Werness, S.; He, J. X.; Cody, W. L.; Doherty, A. M. In vitro assessment of oral delivery for hexapeptide endothelin antagonists. *Life Sci.* 1996, 58, 971-982.
- Kessler, H.; Knot, R. K.; Schmitt, W. Conformational analysis of peptides: Application to drug design. In *NMR Drug Design*; Craik, D. J., Ed.; CRC Press: Boca Raton, FL, 1996; pp 215-244.
- Kessler, H.; Köck, M.; Wein, T.; Gehrke, M. Reinvestigation of the conformation of cyclosporin A in chloroform. *Helv. Chim. Acta* 1990, 73, 1818-1832.
- Kessler, H.; Haessner, R.; Schüller, W. Structure of rapamycin: An NMR and molecular-dynamics investigation. *Helv. Chim. Acta* 1993, 76, 117-130.
- Swindells, D. C.; White, P. S.; Findlay, J. A. The X-ray crystal structure of rapamycin, $C_{15}H_{79}NO_{13}$. *Can. J. Chem.* 1978, 56, 2491-2492.
- Flippen-Anderson, J. L.; Hruby, V. J.; Collins, N.; George, C.; Cudney, B. X-ray structure of $[DPen^2,DPen^4]enkephalin$, a highly potent, δ -opioid receptor selective compound: Comparisons with proposed solution conformations. *J. Am. Chem. Soc.* 1994, 116, 7523-7531.
- Melacini, G.; Zhu, Q.; Goodman, M. Multiconformational NMR analysis of sandostatin (octreotide): Equilibrium between β -sheet and helical structures. *Biochemistry* 1997, 36, 1233-1241.
- Wüthrich, K. *NMR of Proteins and Nucleic Acids*; J. Wiley and Sons: New York, 1984.

(42) Reily, M. D.; Thanabal, V.; Ome, D. O. Structure-induced carbon-13 chemical shifts: A sensitive measure of transient localized secondary structure in peptides. *J. Am. Chem. Soc.* 1992, 114, 6251-6252.

(43) Stewart, J. M.; Young, J. D. *Solid Phase Synthesis*, 2nd ed.; Pierce Chemical Co.: Rockford, IL, 1984.

(44) Bodansky, M.; Bodansky, A. *The Practice of Peptide Synthesis*; Springer-Verlag: Berlin, Germany, 1984.

(45) Mitchell, A. R.; Erickson, B. W.; Ryabtsev, M. N.; Hodges, R. S.; Merrifield, R. B. *Tert*-butoxycarbonylaminoacyl-4-(oxymethyl)-phenylacetamidomethyl-resin, a more acid-resistant support for solid-phase peptide synthesis. *J. Am. Chem. Soc.* 1976, 98, 7357-7562.

(46) Chen, H. G.; Beylin, V. G.; Leja, B.; Goel, O. P. Chiral synthesis of D- and L-3,3-diphenylalanine (DIP), unusual L-amino acids for peptides of biological interest. *Tetrahedron Lett.* 1992, 33, 3293-3296.

(47) Beylin, V. G.; Chen, H. G.; Dunbar, J. B.; Goel, O. P.; Harter, W.; Marlett, M.; Topliss, J. G. Cyclic derivatives of 3,3-diphenylalanine (Dip). II. Novel L-amino acids for peptides of biological interest. *Tetrahedron Lett.* 1992, 34, 953-956.

(48) Knittel, J. J.; He, J. X. Synthesis and resolution of novel 3'-substituted phenylalanine amides. *Pept. Res.* 1990, 3, 176-181.

(49) Sasaki, Y.; Coy, D. H. Solid phase synthesis of peptides containing the CH_2NH peptide bond isostere. *Peptides* 1987, 8, 119-121.

(50) Sasaki, Y.; Murphy, W. A.; Heiman, M. L.; Lance, V. A.; Coy, D. H. Solid-phase synthesis and biological properties of Y[CH₂NH] pseudopeptide analogs of a highly potent somatostatin octapeptide. *J. Med. Chem.* 1987, 30, 1162-1166.

(51) Fehrentz, J. A.; Castro, B. An efficient synthesis of optically active α -(*t*-butoxycarbonylamino)-aldehydes from α -amino acids. *Synthesis* 1983, 676-678.

(52) Kaljuste, K.; Unden, A. New method for the synthesis of N-methyl amino acids containing peptides by reductive methylation of amino groups on the solid phase. *Int. J. Pept. Protein Res.* 1993, 42, 118-124.

(53) Freidinger, R. M.; Hinkle, J. S.; Perlow, D. S. Synthesis of 9-fluorenylmethoxycarbonyl-protected N-alkyl amino acids by reduction of oxazolidinones. *J. Org. Chem.* 1983, 48, 77-81.

(54) Kaiser, E.; Colescott, R. L.; Bossinger, C. D.; Cook, P. I. Color test for detection of free terminal amino groups in the solid-phase synthesis of peptides. *Anal. Biochem.* 1970, 34, 595-598.

(55) Woodley, J. F. Enzymic barriers for GI peptide and protein delivery. *Crit. Rev. Ther. Drug Carrier Syst.* 1994, 11, 61-95.

(56) Cody, W. L.; He, J. X.; Flynn, M. A.; Welch, K. M.; Reynolds, E. E.; Doherty, A. M. Parke-Davis Pharmaceutical Research, Division of Warner-Lambert Co., unpublished results.

(57) Stewart, B. H.; Reyner, E. L.; Tse, E.; Hayes, R. N.; Cody, W. L.; Doherty, A. M. In vitro assessment of oral delivery for hexapeptide endothelin antagonists using stability in intestinal perfusate and Caco-2 permeability. *Pharm. Res.* 1994, 11, S-257.

(58) Artursson, P.; Karlsson, J. Correlation between oral drug absorption in humans and apparent drug permeability coefficients in human intestinal epithelial (Caco-2) cells. *Biochem. Biophys. Res. Commun.* 1993, 175, 880-885.

(59) Hidalgo, I. J.; Raub, R. J.; Borchardt, R. T. Characterization of the human colon carcinoma cell line (Caco-2) as a model system for intestinal epithelial permeability. *Gastroenterology* 1989, 96, 736-749.

(60) Pinto, M.; Robine-Leon, S.; Appay, M. D.; Kedinger, M.; Triadou, N.; Dussaux, E.; Lacroix, B.; Simon-Assmann, P.; Haffen, K.; Fogh, J.; Zweibaum, A. Enterocyte-like differentiation and polarization of the human colon carcinoma cell line Caco-2 in culture. *Biol. Cell* 1983, 47, 232-230.

(61) Watts, C. R.; Tessmer, M. R.; Cody, W. L.; Doherty, A. M.; Kallick, D. A. High resolution NMR structure and molecular dynamics simulation of a potent ET_A and ET_B endothelin receptor antagonist in the presence of dodecylphosphocholine micelles. *Biochemistry* 1997, in press.

(62) Szilagyi, L. Chemical shifts in proteins come of age. *Prog. Nucl. Magn. Reson. Spectrosc.* 1995, 27, 325-443.

(63) Wishart, D. S.; Bigam, C. G.; Holm, A.; Hodges, R. S.; Sykes, B. D. ¹H, ¹³C and ¹⁵N Random coil NMR chemical shifts of the common amino acids. I. Investigations of nearest neighbor effects. *J. Biomol. NMR* 1995, 5, 67-81.

(64) Braunschweiler, L.; Ernst, R. R. Coherence transfer by isotropic mixing: Application to proton correlation spectroscopy. *J. Magn. Reson.* 1983, 53, 521-528.

(65) Rance, M.; Soerensen, O. W.; Bodenhausen, G.; Wagner, G.; Ernst, R. R.; Wüthrich, K. Improved spectral resolution in COSY proton NMR spectra of proteins via double quantum filtering. *Biochem. Biophys. Res. Commun.* 1983, 117, 479-485.

(66) Bothner-By, A. A.; Stephens, R. L.; Lee, J.; Warren, C. D.; Jeanloz, R. W. *J. Am. Chem. Soc.* 1984, 106, 811-813.

(67) Bax, A.; Davis, D. G. Practical aspects of two-dimensional transverse NOE spectroscopy. *J. Magn. Reson.* 1985, 65, 355-360.

(68) Kumar, A.; Ernst, R. R.; Wüthrich, K. A two-dimensional nuclear Overhauser enhancement (2D NOE) experiment for the elucidation of complete proton-proton cross-relaxation networks in biological macromolecules. *Biochem. Biophys. Res. Commun.* 1980, 95, 1-6.

(69) Marion, D.; Wüthrich, K. Application of phase sensitive two-dimensional correlated spectroscopy (COSY) for measurements of proton-proton spin-spin coupling constants in proteins. *Biochem. Biophys. Res. Commun.* 1983, 113, 967-974.

(70) Reily, M. D.; Thanabal, V.; Adams, M. E. The solution structure of ω -Aga-IVB, P-type calcium channel antagonist from venom of the funnel web spider, *Agelenopsis aperta*. *J. Biomol. NMR* 1995, 5, 123-132.

(71) Thanabal, V.; Omeckinsky, D. O.; Reily, M. D.; Cody, W. L. The ¹³C chemical shifts of amino acids in aqueous solution containing organic solvents: Application to the secondary structure characterization of peptides in aqueous trifluoroethanol solution. *J. Biomol. NMR* 1994, 4, 47-59.

(72) Howarth, O. W.; Lilley, D. M. J. Carbon-13 NMR of peptides and proteins. *Prog. Nucl. Magn. Reson. Spectrosc.* 1978, 12, 1-40.

JM970161M